

CERN TH 6924/93
CPT-93 / P.2917
NORDITA-93/43 N,P

**LOW-ENERGY BEHAVIOR OF TWO-POINT FUNCTIONS
OF QUARK CURRENTS**

Johan Bijnens

NORDITA, Blegdamsvej 17
DK-2100 Copenhagen \emptyset , Denmark

Eduardo de Rafael

Centre de Physique Théorique
CNRS - Luminy, Case 907
F 13288 Marseille Cedex 9, France

and

Hanqing Zheng

CERN, CH-1211 Geneva 23, Switzerland

NORDITA-93/43 N,P
CPT-93 / P.2917
CERN-TH 6924/93
May 1993

Abstract

We discuss vector, axial-vector, scalar and pseudoscalar two-point functions at low and intermediate energies. We first review what is known from chiral perturbation theory, as well as from a heat kernel expansion within the context of the extended Nambu-Jona-Lasinio (ENJL) model of ref. [13]. In this work we derive then these two-point functions to all orders in the momenta and to leading order in $1/N_c$. We find an improved high-energy behaviour and a general way of parametrizing them that shows relations between some of the two-point functions, which are also valid in the presence of gluonic interactions. The similarity between the shape of the experimentally known spectral functions and the ones we derive, is greatly improved with respect to those predicted by the usual constituent quark like models. We also obtain the scalar mass $M_S = 2M_Q$ independent of the regularization scheme. In the end, we calculate fully an example of a nonleptonic matrix element in the ENJL-model, the $\pi^+ - \pi^0$ electromagnetic mass difference and find good agreement with the measured value.

1 INTRODUCTION AND REVIEW OF KNOWN RESULTS IN QCD

We shall be concerned with two–point functions of the vector, axial–vector, scalar and pseudoscalar quark currents:

$$V_\mu^{(a)}(x) \equiv \bar{q}(x)\gamma_\mu \frac{\lambda^{(a)}}{\sqrt{2}}q(x) \quad (1)$$

$$A_\mu^{(a)}(x) \equiv \bar{q}(x)\gamma_\mu\gamma_5 \frac{\lambda^{(a)}}{\sqrt{2}}q(x) \quad (2)$$

$$S^{(a)}(x) \equiv -\bar{q}(x) \frac{\lambda^{(a)}}{\sqrt{2}}q(x) \quad (3)$$

$$P^{(a)}(x) \equiv \bar{q}(x)i\gamma_5 \frac{\lambda^{(a)}}{\sqrt{2}}q(x) \quad (4)$$

where $\lambda^{(a)}$ are Gell-Mann $SU(3)$ –matrices acting on the flavour triplets of Dirac spinors: $\bar{q} \equiv (\bar{u}(x), \bar{d}(x), \bar{s}(x))$. Summation over the colour degrees of freedom of the quark fields is understood. These are the quark currents of the QCD Lagrangian with three light flavours u, d, s, in the presence of external vector $v_\mu(x)$, axial vector $a_\mu(x)$, scalar $s(x)$ and pseudoscalar $p(x)$ field matrix sources; i.e.,

$$\mathcal{L}_{QCD}(x) = \mathcal{L}_{QCD}^0 + \bar{q}\gamma_\mu(v_\mu + \gamma_5 a_\mu)q - \bar{q}(s - i\gamma_5 p)q, \quad (5)$$

with

$$\mathcal{L}_{QCD}^0 = -\frac{1}{4} \sum_{A=1}^8 G_{\mu\nu}^{(A)} G^{(A)\mu\nu} + i\bar{q}\gamma^\mu(\partial_\mu + iG_\mu)q \quad (6)$$

and

$$G_\mu \equiv g_s \sum_{A=1}^{N_C^2-1} \frac{\lambda^{(A)}}{2} G_\mu^{(A)}(x) \quad (7)$$

the gluon field matrix in the fundamental $SU(N_C = 3)_{colour}$ representation, with $G_{\mu\nu}^{(A)}$ the gluon field strength tensor

$$G_{\mu\nu}^{(A)}(x) = \partial_\mu G_\nu^{(A)} - \partial_\nu G_\mu^{(A)} - g_s f_{ABC} G_\mu^{(B)} G_\nu^{(C)}, \quad (8)$$

and g_s the colour coupling constant ($\alpha_s = g_s^2/4\pi$).

We want to consider the set of two–point functions:

$$\Pi_{\mu\nu}^V(q)_{ab} = i \int d^4x e^{iq\cdot x} \langle 0 | T (V_\mu^{(a)}(x) V_\nu^{(b)}(0)) | 0 \rangle \quad (9)$$

$$\Pi_{\mu\nu}^A(q)_{ab} = i \int d^4x e^{iq\cdot x} \langle 0 | T (A_\mu^{(a)}(x) A_\nu^{(b)}(0)) | 0 \rangle \quad (10)$$

$$\Pi_\mu^S(q)_{ab} = i \int d^4x e^{iq\cdot x} \langle 0 | T (V_\mu^{(a)}(x) S^{(b)}(0)) | 0 \rangle \quad (11)$$

$$\Pi_\mu^P(q)_{ab} = i \int d^4x e^{iq \cdot x} \langle 0 | T \left(A_\mu^{(a)}(x) P^{(b)}(0) \right) | 0 \rangle \quad (12)$$

$$\Pi^S(q)_{ab} = i \int d^4x e^{iq \cdot x} \langle 0 | T \left(S^{(a)}(x) S^{(b)}(0) \right) | 0 \rangle \quad (13)$$

$$\Pi^P(q)_{ab} = i \int d^4x e^{iq \cdot x} \langle 0 | T \left(P^{(a)}(x) P^{(b)}(0) \right) | 0 \rangle . \quad (14)$$

The relevance of these two–point functions to hadronic physics, within the framework of current algebra, was emphasized a long time ago (See refs.[1] to [4].). With the advent of QCD it became possible to compute the short–distance behavior of these two point functions using perturbation theory in the colour coupling constant because of the property of asymptotic freedom: $\alpha_s(Q^2 \equiv -q^2 \gg \Lambda_{QCD}^2) \sim \log^{-1}(Q^2/\Lambda_{QCD}^2)$, (See refs.[5] to [7].). Non–perturbative corrections at large Q^2 appear as inverse powers in Q^2 [8]. The inclusion of these corrections, combined with a phenomenological ansatz for the corresponding hadronic spectral functions at low energies, has developed into the active field of QCD sum rules. (See e.g. ref.[9] for a review and references therein.) The QCD behaviour of the two point functions above at very low Q^2 values, is controlled by chiral perturbation theory (χ PT). It is important for our later purpose to review here what is known in this respect.

From Lorentz–covariance and SU(3) invariance, the two–point functions above can be decomposed in invariant functions as follows:

$$\Pi_{\mu\nu}^V(q)_{ab} = (q_\mu q_\nu - q^2 g_{\mu\nu}) \Pi_V^{(1)}(Q^2) \delta_{ab} + q_\mu q_\nu \Pi_V^{(0)}(Q^2) \delta_{ab} \quad (15)$$

$$\Pi_{\mu\nu}^A(q)_{ab} = (q_\mu q_\nu - q^2 g_{\mu\nu}) \Pi_A^{(1)}(Q^2) \delta_{ab} + q_\mu q_\nu \Pi_A^{(0)}(Q^2) \delta_{ab} \quad (16)$$

$$\Pi_\mu^S(q)_{ab} = \Pi_M^S(Q^2) q_\mu \delta_{ab} \quad (17)$$

$$\Pi_\mu^P(q)_{ab} = \Pi_M^P(Q^2) i q_\mu \delta_{ab} \quad (18)$$

$$\Pi^S(q)_{ab} = \Pi_S(Q^2) \delta_{ab} \quad (19)$$

$$\Pi^P(q)_{ab} = \Pi_P(Q^2) \delta_{ab} . \quad (20)$$

The low energy behaviour of these invariant functions in $SU(2)_L \times SU(2)_R$ χ PT has been worked out in ref.[10]. It is easy to extend their analysis to $SU(3)_L \times SU(3)_R$ χ PT. In the chiral limit, where the quark mass matrix $\mathcal{M} \rightarrow 0$; and with neglect of chiral loops, which are non leading in the $1/N_C$ –expansion [11], the results are as follows:

$$\Pi_V^{(1)}(Q^2) = -4(2H_1 + L_{10}) + \mathcal{O}(Q^2) \quad (21)$$

$$\Pi_V^{(0)}(Q^2) = 0 \quad (22)$$

$$\Pi_A^{(1)}(Q^2) = \frac{2f_0^2}{Q^2} - 4(2H_1 - L_{10}) + \mathcal{O}(Q^2) \quad (23)$$

$$\Pi_A^{(0)}(Q^2) = 0 \quad (24)$$

$$\Pi_M^S(Q^2) = 0 \quad (25)$$

$$\Pi_M^P(Q^2) = \frac{2B_0f_0^2}{Q^2} \quad (26)$$

$$\Pi^S(Q^2) = 8B_0^2(2L_8 + H_2) + \mathcal{O}(Q^2) \quad (27)$$

$$\Pi^P(Q^2) = \frac{2B_0^2f_0^2}{Q^2} + 8B_0^2(-2L_8 + H_2) + \mathcal{O}(Q^2) . \quad (28)$$

The functions $\Pi_A^{(1)}$, Π_M^P and Π^P get their leading behaviour from the pseudoscalar Goldstone pole. The residue of the pole is proportional to the pion decay constant f_0 ($f_0 \simeq f_\pi = 93.3MeV$). The constant B_0 is related to the vacuum expectation value

$$\langle 0|\bar{q}q|0 \rangle_{|q=u,d,s} = -f_0^2B_0(1 + \mathcal{O}(\mathcal{M})) . \quad (29)$$

The constants L_8 , L_{10} , H_1 and H_2 are coupling constants of the $O(p^4)$ effective chiral Lagrangian in the notation of Gasser and Leutwyler [12]. The constants L_8 and L_{10} are known from the comparison between χ PT and low energy hadron phenomenology. At the scale of the ρ mass:

$$L_8 = (0.9 \pm 0.3) \times 10^{-3} \quad (30)$$

and

$$L_{10} = (-5.5 \pm 0.7) \times 10^{-3} . \quad (31)$$

The constant H_1 and H_2 correspond to couplings which involve external source fields only and therefore cannot be extracted from experiment unambiguously.

It has been recently shown [13] that the extended Nambu Jona-Lasinio model (ENJL-model) describes the values of the low energy parameters rather well. In ref.[13], various relations between the parameters of a low energy effective Lagrangian were obtained that were independant of the input parameters and possible low energy gluonic corrections. Among these was the relation

$$f_V^2 M_V^2 - f_A^2 M_A^2 = f_\pi^2 \quad (32)$$

between couplings and masses of the lowest vector and axial-vector mesons and the pion-decay constant. This corresponds to what is usually called the first Weinberg sum rule [1]. The second Weinberg sum rule, in the lowest resonance saturation form i.e., $f_V^2 M_V^4 = f_A^2 M_A^4$, was, however, not satisfied exactly though the deviation was numerically small. Part of the motivation which triggered our interest in the present work has been to understand the origin of this unsatisfactory result. As we shall show, the low energy expansion method used in ref.[13] is inappropriate to draw conclusions about the intermediate Q^2 -behaviour of two-point functions. The relevant contributions can however be easily summed using a Feynman-diagram expansion of the four fermion couplings in the ENJL-model without introducing collective fields. Section 3 gives the details of this summation method. The same results could be obtained of course using the collective field method, provided though that all higher orders in the Q^2 -expansion were kept.

It is well known that the Weinberg sum rules play a crucial role in the calculation of the electromagnetic $\pi^+ - \pi^0$ mass difference in the chiral limit. In a previous calculation of this mass difference [14] within the framework of the effective action approach [15], it was shown that the quality of the matching between long-distance and short-distance contributions to the photon-loop integral is still rather poor when the vector and axial-vector spectral functions are replaced by constituent quark spectral functions alone. We shall (see also ref.[16]) discuss this problem again in section 4, within the framework of the ENJL-model and with the full Q^2/M_Q^2 dependence summed. This calculation, which as we shall see is rather successful, provides the first non-trivial example of a genuine one loop calculation in the ENJL-model. There are other applications one can now think of doing; in particular calculations at the next to leading order in the $1/N_C$ -expansion. We plan to investigate this in the future.

Throughout this paper we shall work in the chiral limit. The inclusion of corrections, whenever necessary, due to nonzero current quark masses can however be done with the present technology.

The rest of the paper is organized as follows. In section 2 we give an overview of the ENJL-model and the two-point functions in this model in the low-energy limit. We also describe here the parametrization usually used to go beyond the low-energy expansion in this model. Section 3 is the mainstay of this work. Here we derive the two-point functions to all orders in the momenta. We also discuss how gluonic corrections can be included and present numerical results. In the next section we use these two-point functions to calculate completely in the ENJL-model a non-leptonic

matrix-element, the $\pi^+ - \pi^0$ electromagnetic mass difference. In the last section we present our main conclusions. In the appendix we derive the underlying relations that allow for the same type of results for the two-point functions, as those found in ref. [13] for the low-energy constants.

2 TWO-POINT FUNCTIONS IN THE ENJL-MODEL

2.1 A brief review of the ENJL-model

The scenario suggested in ref.[13], assumes that at intermediate energies below or of the order of the spontaneous chiral symmetry breaking scale Λ_χ , the Lagrangian of the ENJL-model is a good effective realization of the standard QCD Lagrangian i.e.,

$$\mathcal{L}_{QCD} \rightarrow \mathcal{L}_{QCD}^{*\chi} + \mathcal{L}_{NJL}^{S,P} + \mathcal{L}_{NJL}^{V,A} + \mathcal{O}\left(\frac{1}{\Lambda_\chi^4}\right) \quad (33)$$

with

$$\mathcal{L}_{NJL}^{S,P}(x) = \frac{8\pi^2 G_S(\Lambda_\chi)}{N_c \Lambda_\chi^2} \sum_{a,b} (\bar{q}_R^a q_L^b)(\bar{q}_L^b q_R^a) \quad (34)$$

and

$$\mathcal{L}_{NJL}^{V,A}(x) = -\frac{8\pi^2 G_V(\Lambda_\chi)}{N_c \Lambda_\chi^2} \sum_{a,b} [(\bar{q}_L^a \gamma^\mu q_L^b)(\bar{q}_L^b \gamma_\mu q_L^a) + (L \rightarrow R)]. \quad (35)$$

Here a and b are u, d, s flavour indices and colour summation within each quark bilinear bracket is implicit; $q_L = \frac{1}{2}(1 - \gamma_5)q(x)$ and $q_R = \frac{1}{2}(1 + \gamma_5)q(x)$. The couplings G_S and G_V are dimensionless quantities. In principle they are calculable functions of the ratio of the cut-off scale Λ_χ to the renormalization scale $\Lambda_{\overline{MS}}$. In practice the calculation requires knowledge of the non-perturbative behaviour of QCD and G_S and G_V will be taken as independent unknown constants. In choosing the forms (34) and (35) of these four quark operators we have only kept those couplings that are allowed by the symmetries of the original QCD Lagrangian, and which are leading in the $1/N_C$ -expansion [11]. With one inverse power of N_C pulled-out, both couplings G_S and G_V are $\mathcal{O}(1)$ in the large N_C limit. The Λ_χ index in $\mathcal{L}_{QCD}^{\Lambda_\chi}$ means that only the low frequency modes of the quark and gluon fields are to be included.

The basic assumption in considering the ENJL-model as a good effective Lagrangian of QCD is that at intermediate energies below or of the order of the spontaneous chiral symmetry breaking scale, the operators $\mathcal{L}_{NJL}^{S,P}$ and $\mathcal{L}_{NJL}^{V,A}$ are the leading operators of higher dimension which, due to the growing of their couplings G_S and G_V as the ultraviolet cut-off approaches its critical value from above, become relevant or marginal.

As is well known in the Nambu Jona-Lasinio model [17], the $\mathcal{L}_{NJL}^{S,P}$ operator, for values of $G_S > 1$, is at the origin of the the spontaneous chiral symmetry breaking.

It is this operator which generates a constituent chiral quark mass term (U is a unitary 3×3 matrix which collects the pseudoscalar Goldstone field modes):

$$- M_Q(\bar{q}_L U^\dagger q_R + \bar{q}_R U q_L) = -M_Q \bar{Q} Q , \quad (36)$$

like the one which appears in the Georgi–Manohar model [18]; as well as in the effective action approach of ref.[15].

As discussed in ref.[13], the $\mathcal{L}_{NJL}^{V,A}$ operator is at the origin of an effective axial coupling of the constituent quark fields $Q(x)$ with the Goldstone modes

$$\frac{i}{2} g_A \bar{Q} \gamma^\mu \gamma_5 \xi_\mu Q , \quad (37)$$

with

$$g_A = \frac{1}{1 + 4G_V \epsilon \Gamma(0, \epsilon)} , \quad \epsilon \equiv M_Q^2 / \Lambda_\chi^2 \quad (38)$$

and $\Gamma(0, \epsilon)$ the incomplete gamma function:

$$\Gamma(0, \epsilon) = \int_\epsilon^\infty \frac{dz}{z} e^{-z} . \quad (39)$$

For ϵ small,

$$\Gamma(0, \epsilon) = -\log \epsilon - \gamma_E + \mathcal{O}(\epsilon) , \quad (40)$$

with $\gamma_E = 0.5772 \dots$, Euler's constant. We recall that in eq. (37)

$$\xi_\mu = i \left\{ \xi^\dagger [\partial_\mu - i(v_\mu + a_\mu)] \xi - \xi [\partial_\mu - i(v_\mu - a_\mu)] \xi^\dagger \right\} ; \quad (41)$$

with

$$U = \xi \xi \quad (42)$$

and

$$Q = Q_L + Q_R \quad (43)$$

$$Q_L = \xi q_L , \quad Q_R = \xi^\dagger q_R . \quad (44)$$

The appearance of incomplete gamma functions is due to the proper time regularization which is used in calculating the fermion determinant via the Seeley–De Witt expansion. The type of integrals which appear are ($\epsilon = M_Q^2 / \Lambda_\chi^2$)

$$\begin{aligned} \int_{1/\Lambda_\chi^2}^\infty \frac{d\tau}{\tau} \frac{1}{16\pi^2 \tau^2} \tau^n e^{-\tau M_Q^2} &= \frac{1}{16\pi^2} \frac{1}{(M_Q^2)^{n-2}} \int_\epsilon^\infty \frac{dz}{z} e^{-z} z^{n-2} \\ &= \frac{1}{16\pi^2} \frac{1}{(M_Q^2)^{n-2}} \Gamma(n-2, \epsilon) ; \\ n &= 1, 2, 3, \dots \end{aligned} \quad (45)$$

The result for the axial coupling g_A in eq. (38) is the result to leading order in the $1/N_C$ -expansion. In terms of Feynman diagrams it can be understood as the infinite sum of constituent quark bubbles shown in Fig.1a, where the cross at the end represents the pion field. These are the diagrams generated by the G_V – four fermion coupling to leading order in the $1/N_C$ -expansion [19]. The quark propagators in Fig.1a are constituent quark propagators, solutions of the Schwinger–Dyson equation in the large N_C approximation, which diagrammatically is represented in Fig.1b.

In its simplest version where one assumes furthermore that all the relevant gluonic effects for low energy physics can be absorbed in the couplings G_S and G_V , the ENJL-model has only three free parameters: G_S , G_V and Λ_χ . We find it useful to specify these in terms of M_Q , Λ_χ and g_A instead. For this purpose one should remember that ($\epsilon = M_Q^2/\Lambda_\chi^2$)

$$G_S^{-1} = \epsilon\Gamma(-1, \epsilon) = e^{-\epsilon} - \epsilon\Gamma(0, \epsilon) . \quad (46)$$

2.2 Low Q^2 -behaviour of two-point functions in the ENJL-model.

As we discussed in the previous section, the low-energy behaviour of two point function quark currents, is governed by the constants f_π^2 , B_0 , L_8 , L_{10} , H_1 and H_2 . In the ENJL-model, these constants have been calculated in ref.[13] with the results ($\epsilon = M_Q^2/\Lambda_\chi^2$):

$$f_\pi^2 = \frac{N_C}{16\pi^2} 4M_Q^2 g_A \Gamma(0, \epsilon) \quad (47)$$

$$2H_1 + L_{10} = -\frac{N_C}{16\pi^2} \frac{1}{3} \Gamma(0, \epsilon) \quad (48)$$

$$2H_1 - L_{10} = -\frac{N_C}{16\pi^2} g_A^2 \frac{1}{3} [\Gamma(0, \epsilon) - \Gamma(1, \epsilon)] \quad (49)$$

$$L_8 = \frac{N_C}{16\pi^2} \frac{1}{16} g_A^2 \left[\Gamma(0, \epsilon) - \frac{2}{3} \Gamma(1, \epsilon) \right] \quad (50)$$

$$H_2 = \frac{N_C}{16\pi^2} \frac{1}{8} g_A^2 \left[\left(1 - 4 \frac{\Gamma(0, \epsilon)}{\Gamma(-1, \epsilon)} \right) \Gamma(0, \epsilon) + \frac{2}{3} \Gamma(1, \epsilon) \right] . \quad (51)$$

In fact, the calculations made in ref.[13] suggest a possible improvement of the invariant functions in eqs. (21) to (28) when the contribution from the corresponding resonance propagators is also taken into account, with the results

$$\Pi_V^{(1)}(Q^2) = -4(2H_1 + L_{10}) - \frac{2f_V^2 Q^2}{M_V^2 + Q^2} , \quad (52)$$

$$\Pi_A^{(1)}(Q^2) = \frac{2f_\pi^2}{Q^2} - 4(2H_1 - L_{10}) - \frac{2f_A^2 Q^2}{M_A^2 + Q^2} , \quad (53)$$

and

$$\Pi^S(Q^2) = 8B_0^2 \left\{ 2\tilde{L}_8 + \tilde{H}_2 + \frac{2c_m^2}{Q^2 + M_S^2} \right\} . \quad (54)$$

For the other invariant functions, the results are the same as in eqs. (21) to (28) with the parameter values given in eqs. (47) to (51). Several comments on these results are in order:

i) Two relations which follow from the ENJL-model [13] are

$$2H_1 - L_{10} = -f_A^2/2 \quad \text{and} \quad 2H_1 + L_{10} = -f_V^2/2 . \quad (55)$$

These relations are of the same type as the first Weinberg sum rule relation in eq. (32) i.e., they are independent of the input parameters and possible low energy gluonic corrections. As first shown in ref.[20], they are crucial to ensure that the low energy effective theory is compatible with the known short-distance properties of the underlying theory – QCD. It is reassuring that the ENJL-model indeed respects these constraints. Using these relations, we can also write $\Pi_V^{(1)}$ and $\Pi_A^{(1)}$ in the form

$$\Pi_V^{(1)} = \frac{2f_V^2 M_V^2}{M_V^2 + Q^2} , \quad (56)$$

$$\Pi_A^{(1)} = \frac{2f_\pi^2}{Q^2} + \frac{2f_A^2 M_A^2}{M_A^2 + Q^2} ; \quad (57)$$

a form much more similar to the usual vector meson dominance (VMD) phenomenological parametrizations found in the literature.

ii) The constant c_m in eq. (54) denotes the coupling

$$c_m \text{tr} \left(S(x) \left[\xi^\dagger \chi \xi^\dagger + \xi \chi^\dagger \xi \right] \right) \quad (58)$$

in the effective scalar Lagrangian. Here

$$\chi = 2B_0 [s(x) + ip(x)] , \quad (59)$$

with $s(x)$ and $p(x)$ the external scalar and pseudoscalar matrix field sources. As discussed in ref.[13], the couplings L_8 and H_2 receive contributions both from the quark loop – which we denote \tilde{L}_8 and \tilde{H}_2 – and from the integration of scalar fields – which we denote L_8^S and H_2^S ; i.e.,

$$L_8 = \tilde{L}_8 + L_8^S \quad \text{and} \quad H_2 = \tilde{H}_2 + H_2^S . \quad (60)$$

In fact

$$\frac{2c_m^2}{M_S^2} = 2L_8^S + H_2^S = 2H_2^S = \frac{N_C}{16\pi^2} \frac{1}{4} g_A^2 \frac{\Gamma(0, \epsilon)}{\Gamma(-1, \epsilon)^2} [\Gamma(-1, \epsilon) - 2\Gamma(0, \epsilon)]^2 . \quad (61)$$

iii) Equations (52), (53) and (54) imply a specific form of the resummation to all orders in an expansion in powers of Q^2 . As we shall see, this is not however the correct form which follows from the exact resummation of Feynman diagrams, to leading order in the $1/N_C$ -expansion.

We shall finally give the expressions for the masses M_S , M_V and M_A which are obtained in the ENJL-model in ref.[13]:

$$M_S^2 = 4M_Q^2 \frac{1}{1 - \frac{2}{3} \frac{\Gamma(1, \epsilon)}{\Gamma(0, \epsilon)}} , \quad (62)$$

$$M_V^2 = \frac{3}{2} \frac{\Lambda_\chi^2}{G_V} \frac{1}{\Gamma(0, \epsilon)} = 6M_Q^2 \frac{g_A}{1 - g_A} , \quad (63)$$

$$M_A^2 = 6M_Q^2 \frac{1}{1 - g_A} \frac{1}{1 - \frac{\Gamma(1, \epsilon)}{\Gamma(0, \epsilon)}} . \quad (64)$$

3 FULL Q^2 -DEPENDENT TWO-POINT FUNCTIONS IN THE ENJL-MODEL

3.1 The Vector Two-Point Function

To illustrate the method, we shall first discuss with quite a lot of detail the vector invariant function $\Pi_V^{(1)}(Q^2)$. In the ENJL-model, and to leading order in the $1/N_C$ -expansion, we have to sum over the infinite class of bubble diagrams shown in Fig. 2a. Algebraically, this corresponds to the sum

$$(q^\mu q^\nu - q^2 g^{\mu\nu}) \overline{\Pi}_V^{(1)} + (q^\mu q^\alpha - q^2 g^{\mu\alpha}) \overline{\Pi}_V^{(1)} \left(\frac{-4\pi^2 G_V}{N_C \Lambda_\chi^2} \right) \times 2(q_\alpha q^\nu - q^2 g_\alpha^\nu) \overline{\Pi}_V^{(1)} + \dots , \quad (65)$$

where the explicit factor of 2 in the second term comes from the two possible contractions between the fermion fields of the vector four-quark operator. The overall result is

$$(q^\mu q^\nu - q^2 g^{\mu\nu}) \left\{ \overline{\Pi}_V^{(1)} + \overline{\Pi}_V^{(1)} q^2 \frac{8\pi^2 G_V}{N_C \Lambda_\chi^2} \overline{\Pi}_V^{(1)} + \dots \right\} . \quad (66)$$

Notice that for this two-point function, only the vector four quark interaction with coupling G_V can contribute. No mixing between different operators can occur in this case. The one loop bubble in Fig.2b corresponds to the bare fermion-loop diagram of the mean field approximation defined in ref.[13], which in what follows we shall denote with an overlined expression

$${}^1\Pi_V^{(1)}(Q^2) = \overline{\Pi}_V^{(1)}(Q^2) . \quad (67)$$

It is easy to see that at the n -loop bubble level, the corresponding expression for ${}^n\Pi_V^{(1)}(Q^2)$ will be given by the $n - 1$ - loop bubble result multiplied by the coupling

G_V and one more factor of the one-loop result, i.e.,

$${}^n\Pi_V^{(1)}(Q^2) = {}^{n-1}\Pi_V^{(1)}(Q^2) \frac{8\pi^2 G_V}{N_C \Lambda_\chi^2} (-Q^2) \bar{\Pi}_V^{(1)}(Q^2) . \quad (68)$$

This series can then be summed with the result

$$\Pi_V^{(1)} = \frac{\bar{\Pi}_V^{(1)}(Q^2)}{1 + Q^2 \frac{8\pi^2 G_V}{N_C \Lambda_\chi^2} \bar{\Pi}_V^{(1)}(Q^2)} . \quad (69)$$

We discuss next the calculation of $\bar{\Pi}_V^{(1)}(Q^2)$ in some detail. The spectral function associated to $\bar{\Pi}_V^{(1)}(Q^2)$ is the one corresponding to the $Q\bar{Q}$ intermediate state in a P-wave and can be calculated unambiguously with the well known result

$$\frac{1}{\pi} \text{Im} \bar{\Pi}_V^{(1)}(t) = \frac{N_C}{16\pi^2} \frac{4}{3} \left(1 + \frac{2M_Q^2}{t} \right) \sqrt{1 - \frac{4M_Q^2}{t}} \theta(t - 4M_Q^2) . \quad (70)$$

The function $\bar{\Pi}_V^{(1)}(Q^2)$ we seek for has to obey three criteria:

- i) It must obey the relevant Ward identities.
 - ii) Its discontinuity should coincide with the spectral function in eq. (70).
 - iii) When expanded in powers of Q^2 it must reproduce the heat kernel calculation of the effective action approach, with the same proper time regularization results.
- These three criteria will in fact apply to all the two-point functions we discuss.

To proceed with the calculation of $\bar{\Pi}_V^{(1)}(Q^2)$, we write a once subtracted dispersion relation for this function

$$\bar{\Pi}_V^{(1)}(Q^2) = \bar{\Pi}_V^{(1)}(0) - Q^2 \int_0^\infty \frac{dt}{t} \frac{1}{t + Q^2} \frac{1}{\pi} \text{Im} \bar{\Pi}_V^{(1)}(t) . \quad (71)$$

Requirement iii) implies that $\bar{\Pi}_V^{(1)}(0)$ is fixed, with the result ($\epsilon = M_Q^2/\Lambda_\chi^2$)

$$\bar{\Pi}_V^{(1)}(0) = \frac{N_C}{16\pi^2} \frac{4}{3} \Gamma(0, \epsilon) . \quad (72)$$

With $\frac{1}{\pi} \text{Im} \bar{\Pi}_V^{(1)}(t)$ in eq. (70) inserted in the integrand of the r.h.s. of eq. (71); and with the successive change of variables

$$\frac{4M_Q^2}{t} = 1 - y^2 \quad \text{and} \quad y = 1 - 2x , \quad (73)$$

we have that

$$\int_0^\infty \frac{dt}{t} \frac{Q^2}{t + Q^2} \frac{1}{\pi} \text{Im} \bar{\Pi}_V^{(1)}(t) = \frac{N_C}{16\pi^2} \frac{2}{3} \int_0^1 dx (1 - 2x)^2 [1 + 2x(1 - x)] \frac{Q^2}{M_Q^2 + Q^2 x(1 - x)} . \quad (74)$$

In order to match with the proper time regularization which has been used in the calculation of $\bar{\Pi}_V^{(1)}(0)$, we next replace the denominator in the r.h.s. of eq. (74) as follows

$$\frac{1}{M_Q^2 + Q^2 x(1-x)} \rightarrow \int_{1/\Lambda_\chi^2}^{\infty} d\tau e^{-\tau[M_Q^2 + Q^2 x(1-x)]} . \quad (75)$$

Performing an integration by parts in the x -variable we then finally get the result ($\epsilon = M_Q^2/\Lambda_\chi^2$)

$$\int_0^\infty \frac{dt}{t} \frac{Q^2}{t+Q^2} \frac{1}{\pi} \text{Im} \bar{\Pi}_V^{(1)}(t) = \frac{N_C}{16\pi^2} \frac{4}{3} \left\{ \Gamma(0, \epsilon) - 6 \int_0^1 dx x(1-x) \Gamma(0, x_Q) \right\} \quad (76)$$

where x_Q is a short-hand notation, which we shall use from here onwards, for

$$x_Q = \frac{M_Q^2 + Q^2 x(1-x)}{\Lambda_\chi^2} . \quad (77)$$

Combining eqs. (71), (72) and (76), we obtain

$$\bar{\Pi}_V^{(1)}(Q^2) = \frac{N_C}{16\pi^2} 8 \int_0^1 dx x(1-x) \Gamma(0, x_Q) . \quad (78)$$

The first few terms in a Q^2 -expansion of this expression are

$$\bar{\Pi}_V^{(1)}(Q^2) = \frac{N_C}{16\pi^2} \left\{ \frac{4}{3} \Gamma(0, \epsilon) - \frac{4}{15} \Gamma(1, \epsilon) \frac{Q^2}{M_Q^2} + \frac{1}{35} \Gamma(2, \epsilon) \frac{Q^4}{M_Q^4} + \mathcal{O}(Q^6) \right\} , \quad (79)$$

in agreement with the proper time regularized heat kernel effective action result.

The imaginary part of $\bar{\Pi}_V^{(1)}(Q^2)$ evaluated from eq. (78) using the $i\epsilon$ prescription $x_Q \rightarrow (M_Q^2 + Q^2 x(1-x) - i\epsilon)/\Lambda_\chi^2$ in the log term: $\Gamma(0, x_Q) = -\log x_Q - \gamma_E + \mathcal{O}(x_Q)$, reproduces the spectral function in eq. (70).

We shall now try to cast the result for $\Pi_V^{(1)}(Q^2)$ in eq. (69) in the simple VMD-form of eq.(56):

$$\Pi_V^{(1)}(Q^2) = \frac{N_C \Lambda_\chi^2 / 8\pi^2 G_V}{(\bar{\Pi}_V^{(1)})^{-1} \frac{N_C \Lambda_\chi^2}{8\pi^2 G_V} + Q^2} = \frac{2f_V^2(Q^2) M_V^2(Q^2)}{M_V^2(Q^2) + Q^2} , \quad (80)$$

where we have set

$$2f_V^2(Q^2) M_V^2(Q^2) = \frac{N_C \Lambda_\chi^2}{8\pi^2 G_V} , \quad (81)$$

and

$$M_V^2(Q^2) = \frac{\Lambda_\chi^2}{4G_V} \frac{1}{\int_0^1 dx x(1-x) \Gamma(0, x_Q)} . \quad (82)$$

We find that the full Q^2 -dependent vector two-point function can indeed be cast in the VMD-form of eq. (56) provided that the coupling parameters $f_V(Q^2)$ and

$M_V(Q^2)$ become Q^2 dependent. Their value at $Q^2 = 0$ happen to coincide, in this case, with the couplings in the low energy effective Lagrangian i.e.,

$$M_V^2(Q^2 = 0) = M_V^2 = \frac{3}{2} \frac{\Lambda_\chi^2}{G_V} \frac{1}{\Gamma(0, \epsilon)} . \quad (83)$$

and

$$f_V^2(Q^2 = 0) = f_V^2 = \frac{N_C}{16\pi^2} \frac{2}{3} \Gamma(0, \epsilon) . \quad (84)$$

The product $f_V^2(Q^2)M_V^2(Q^2)$ is scale-invariant.

In order to see the hadronic content of the full vector two-point function we propose to examine the complete spectral function

$$\frac{1}{\pi} \text{Im} \Pi_V^{(1)}(t) = \frac{\frac{1}{\pi} \text{Im} \bar{\Pi}_V^{(1)}(t)}{\left[1 - t \frac{8\pi^2 G_V}{N_C \Lambda_\chi^2} \text{Re} \bar{\Pi}_V^{(1)}(t) \right]^2 + \left[t \frac{8\pi^2 G_V}{N_C \Lambda_\chi^2} \text{Im} \bar{\Pi}_V^{(1)}(t) \right]^2} \quad (85)$$

and plot it as a function of t for the input parameter values

$$M_Q = 265 \text{MeV}, \quad \Lambda_\chi = 1165 \text{MeV} \quad (86)$$

and

$$g_A = 0.61 . \quad (87)$$

These are the values corresponding to fit #1 in ref.[13]. The plot is the one shown in Fig. 3 (the full line). For the sake of comparison, we have also plotted in the same figure the spectral function $\frac{1}{\pi} \text{Im} \bar{\Pi}_V^{(1)}(t)$ corresponding to the mean field approximation (the dashed line). The improvement towards a reasonable simulation of the well known experimental shape of the $J^P = 1^-, I = 1$ hadronic spectral function is rather notorious.

3.2 The Axial-Vector Two-Point Function

The infinite series of bubble diagrams we have to sum in this case is formally very similar to the one already discussed in the previous subsection. Again, only the vector four-quark interaction with coupling G_V contributes in this case with the result

$$\Pi_A^{(1)}(Q^2) = \frac{\bar{\Pi}_A^{(1)}(Q^2)}{1 + Q^2 \frac{8\pi^2 G_V}{N_C \Lambda_\chi^2} \bar{\Pi}_A^{(1)}(Q^2)} . \quad (88)$$

The axial two-point function $\bar{\Pi}_A^{\mu\nu}(q)$ in the mean field approximation, has however more structure than the corresponding vector two-point function because now, due to the presence of a constituent quark mass, the axial invariant function $\bar{\Pi}_A^{(0)}$ in the decomposition corresponding to eq. (16) doesn't vanish. Both $\bar{\Pi}_A^{(1)}(Q^2)$ and $\bar{\Pi}_A^{(0)}(Q^2)$

have associated spectral functions which can be calculated unambiguously with the results:

$$\frac{1}{\pi} \text{Im} \bar{\Pi}_A^{(1)}(t) = \frac{N_C}{16\pi^2} \frac{4}{3} \left(1 - \frac{4M_Q^2}{t}\right) \sqrt{1 - \frac{4M_Q^2}{t}} \theta(t - 4M_Q^2) \quad (89)$$

$$\frac{1}{\pi} \text{Im} \bar{\Pi}_A^{(0)}(t) = \frac{N_C}{16\pi^2} \frac{8M_Q^2}{t} \sqrt{1 - \frac{4M_Q^2}{t}} \theta(t - 4M_Q^2) \quad (90)$$

Notice that the three spectral functions $\frac{1}{\pi} \text{Im} \bar{\Pi}_V^{(1)}(t)$, $\frac{1}{\pi} \text{Im} \bar{\Pi}_A^{(1)}(t)$ and $\frac{1}{\pi} \text{Im} \bar{\Pi}_A^{(0)}(t)$ satisfy the identity:

$$\frac{1}{\pi} \text{Im} \bar{\Pi}_V^{(1)}(t) - \frac{1}{\pi} \text{Im} \bar{\Pi}_A^{(1)}(t) - \frac{1}{\pi} \text{Im} \bar{\Pi}_A^{(0)}(t) = 0 . \quad (91)$$

In fact this is nothing but a particular case of a general Ward identity which two-point functions in the mean field approximation must obey:

$$\bar{\Pi}_V^{(1)}(Q^2) - \bar{\Pi}_A^{(1)}(Q^2) - \bar{\Pi}_A^{(0)}(Q^2) = 0 . \quad (92)$$

The proof of this identity can be found in the Appendix. It is precisely this identity which guarantees that the first Weinberg sum rule in the mean field approximation is automatically satisfied.

From the asymptotic behaviour of $\text{Im} \bar{\Pi}_A^{(0)}(t)$ in eq. (90) we conclude that the dispersive part of the function $\bar{\Pi}_A^{(0)}(Q^2)$ obeys an unsubtracted dispersion relation. To this we have to add the pole term calculated in the effective action approach i.e.,

$$\bar{\Pi}_A^{(0)}(Q^2) = \frac{-2\bar{f}_\pi^2}{Q^2} + \int_0^\infty \frac{dt}{t+Q^2} \frac{1}{\pi} \text{Im} \bar{\Pi}_A^{(0)}(t) , \quad (93)$$

with $(\epsilon = M_Q^2/\Lambda_\chi^2)$

$$\bar{f}_\pi^2 = \frac{N_C}{16\pi^2} 4M_Q^2 \Gamma(0, \epsilon) . \quad (94)$$

Using the same change of variables as in eqs. (73), we obtain

$$\int_0^\infty \frac{dt}{t+Q^2} \frac{1}{\pi} \text{Im} \bar{\Pi}_A^{(0)}(t) = \frac{N_C}{16\pi^2} 4M_Q^2 \int_0^1 dx (1-2x)^2 \frac{1}{M_Q^2 + Q^2 x(1-x)} . \quad (95)$$

Next, we use the same proper time representation for the denominator in the right hand side as in eq. (75), and perform an integration by parts in the x -variable, with the result

$$\int_0^\infty \frac{dt}{t+Q^2} \frac{1}{\pi} \text{Im} \bar{\Pi}_A^{(0)}(t) = \frac{N_C}{16\pi^2} \frac{8M_Q^2}{Q^2} \left[\Gamma(0, \epsilon) - \int_0^1 dx \Gamma(0, x_Q) \right] , \quad (96)$$

with x_Q defined in eq. (77). Inserting this result in the r.h.s. of eq. (93) leads to the final result

$$\bar{\Pi}_A^{(0)}(Q^2) = -\frac{N_C}{16\pi^2} \frac{8M_Q^2}{Q^2} \int_0^1 dx \Gamma(0, x_Q) \equiv -\frac{2\bar{f}_\pi^2(Q^2)}{Q^2} , \quad (97)$$

which defines a running $\bar{f}_\pi(Q^2)$ in the mean field approximation. The first few terms in a Q^2 -expansion of $\bar{f}_\pi(Q^2)$ are

$$\bar{f}_\pi(Q^2) = \frac{N_C}{16\pi^2} 4M_Q^2 \left\{ \Gamma(0, \epsilon) - \frac{1}{6} \Gamma(1, \epsilon) \frac{Q^2}{M_Q^2} + \mathcal{O}(Q^4) \right\}, \quad (98)$$

in agreement with the proper time regularized heat kernel effective action result.

Once we have calculated $\bar{\Pi}_A^{(0)}(Q^2)$ and $\bar{\Pi}_V^{(1)}(Q^2)$, the function $\bar{\Pi}_A^{(1)}(Q^2)$ follows from the Ward identity in eq. (92) with the result

$$\bar{\Pi}_A^{(1)}(Q^2) = \frac{N_C}{16\pi^2} 8 \left\{ \frac{M_Q^2}{Q^2} \int_0^1 dx \Gamma(0, xQ) + \int_0^1 dx x(1-x) \Gamma(0, xQ) \right\}. \quad (99)$$

It is nevertheless instructive to calculate $\bar{\Pi}_A^{(1)}(Q^2)$ independently as an illustration of the method we are using. First we observe that the dispersive part of $\bar{\Pi}_A^{(1)}(Q^2)$ needs a subtraction. On the other hand, we know from the effective action calculation that $\bar{\Pi}_A^{(1)}(Q^2)$ has a pole term (see eqs. (53) and (49))

$$\bar{\Pi}_A^{(1)}(Q^2) = \frac{2\bar{f}_\pi^2}{Q^2} - \frac{N_C}{16\pi^2} \frac{4}{3} \Gamma(1, \epsilon) + \frac{N_C}{16\pi^2} \frac{4}{3} \Gamma(0, \epsilon) + \mathcal{O}(Q^2). \quad (100)$$

We recognize the second term in the r.h.s. of this expression as the constant term in the Q^2 -expansion of $\bar{f}_\pi^2(Q^2)$ in eq. (98), which means that the subtraction constant needed for the dispersion relation is only the third term. However this term is precisely the same as the one corresponding to the vector function $\Pi_V^{(1)}(0)$ in eq. (72). We must therefore separate the spectral function $\frac{1}{\pi} \text{Im} \Pi_A^{(1)}(t)$ in two pieces: one which reproduces the vector spectral function $\frac{1}{\pi} \text{Im} \Pi_V^{(1)}(t)$, for which we shall write a once subtracted dispersion and the rest. But this is precisely the Ward identity separation we already pointed out in eq. (91). We then have

$$\begin{aligned} \Pi_A^{(1)}(Q^2) &= \frac{2\bar{f}_\pi^2}{Q^2} - \frac{N_C}{16\pi^2} \int_0^\infty \frac{dt}{t+Q^2} \frac{8M_Q^2}{t} \sqrt{1 - \frac{4M_Q^2}{t}} \theta(t - 4M_Q^2) + \frac{N_C}{16\pi^2} \frac{4}{3} \Gamma(0, \epsilon) \\ &\quad - \frac{N_C}{16\pi^2} \frac{4}{3} \int_0^\infty \frac{dt}{t} \frac{Q^2}{t+Q^2} \left(1 + \frac{2M_Q^2}{t} \right) \sqrt{1 - \frac{4M_Q^2}{t}} \theta(t - 4M_Q^2). \end{aligned} \quad (101)$$

the two dispersive integrals are those calculated before in eq. (96) for the unsubtracted piece. Putting these results together leads to the result in eq. (99).

With these results in hand, we shall now try to cast $\Pi_A^{(1)}(Q^2)$ in eq. (88) as close as possible to the VMD-form of eq. (57):

$$\Pi_A^{(1)}(Q^2) = \frac{\bar{\Pi}_V^{(1)} - \bar{\Pi}_A^{(0)}}{1 - Q^2 \frac{8\pi^2 G_V}{N_C \Lambda_\chi^2} \bar{\Pi}_A^{(0)} + Q^2 \frac{8\pi^2 G_V}{N_C \Lambda_\chi^2} \bar{\Pi}_V^{(1)}}. \quad (102)$$

From the calculated expression for $\overline{\Pi}_A^{(0)}(Q^2)$ in eq. (97), it follows that

$$1 - Q^2 \frac{8\pi^2 G_V}{N_C \Lambda_\chi^2} \overline{\Pi}_A^{(0)}(Q^2) = 1 + 4G_V \frac{M_Q^2}{\Lambda_\chi^2} \int_0^1 dx \Gamma(0, x_Q) . \quad (103)$$

At $Q^2 = 0$, the r.h.s. is precisely g_A^{-1} (see eq. (38)). This is not a surprising result. The evaluation of the axial vector form factor of a constituent chiral quark from the infinite series of bubble graphs in Fig. 1a, leads to the result

$$g_A(Q^2) = \frac{1}{1 + (G_V/\Lambda_\chi^2) 4M_Q^2 \int_0^1 dx \Gamma(0, x_Q)} , \quad (104)$$

which at $Q^2 = 0$ coincides with the axial coupling constant g_A obtained in the calculation of the low energy effective action in ref.[13]. Using this result, we can now rewrite the r.h.s. of eq. (102) in the following simple form:

$$\overline{\Pi}_A^{(1)}(Q^2) = \frac{2f_\pi^2(Q^2)}{Q^2} + \frac{2f_A^2(Q^2)M_A^2(Q^2)}{M_A^2(Q^2) + Q^2} , \quad (105)$$

where

$$f_\pi^2(Q^2) = g_A(Q^2) \bar{f}_\pi^2(Q^2) ; \quad (106)$$

$$M_A^2(Q^2) = \frac{1}{g_A(Q^2)} M_V^2(Q^2) ; \quad (107)$$

and

$$f_A^2(Q^2) = g_A^2(Q^2) f_V^2(Q^2) , \quad (108)$$

with $\bar{f}_\pi^2(Q^2)$, $M_V^2(Q^2)$ and $f_V^2(Q^2)$ as given in eqs. (97), (82) and (81), respectively. Notice that at $Q^2 = 0$

$$f_\pi^2(Q^2 = 0) = f_\pi^2 = \frac{N_C}{16\pi^2} 4M_Q^2 g_A \Gamma(0, \epsilon) ; \quad (109)$$

i.e., the same expression which appears in the low energy effective action; however $M_A^2(Q^2 = 0)$ and $f_A^2(Q^2 = 0)$ do not coincide with the expressions for the couplings M_A^2 and f_A^2 as given in eqs. (64) and (55), (49). We now have instead

$$M_A^2(Q^2 = 0) = \frac{1}{g_A} M_V^2 \quad \text{and} \quad f_A^2(Q^2 = 0) = g_A^2 f_V^2 . \quad (110)$$

The remarkable new result is that now, in terms of the running couplings and running masses, both the first and second Weinberg sum rule are satisfied

$$f_V^2(Q^2) M_V^2(Q^2) = f_A^2(Q^2) M_A^2(Q^2) + f_\pi^2(Q^2) \quad (111)$$

and

$$f_V^2(Q^2) M_V^4(Q^2) = f_A^2(Q^2) M_A^4(Q^2) . \quad (112)$$

The fact that $f_A^2(Q^2 = 0)$ does not coincide with the f_A^2 defined in the effective action approach can be understood from a comparison between eqs. (57) and eqs. (105). Both expressions coincide to $\mathcal{O}(Q^2)$:

$$\Pi_A^{(1)}|_{eq. (57)} = \frac{2f_\pi^2}{Q^2} + 2f_A^2 + \mathcal{O}(Q^2) \quad (113)$$

$$\Pi_A^{(1)}|_{eq. (105)} = \frac{2f_\pi^2}{Q^2} - \frac{N_C}{16\pi^2} \frac{4}{3} g_A^2 \Gamma(1, \epsilon) + 2f_A^2(Q^2 = 0) + \mathcal{O}(Q^2) \quad (114)$$

It is the fact that part of the constant term is reabsorbed in the Q^2 -dependence of f_π^2 , that is at the origin of this difference. The precise relation is

$$f_A^2 = f_A^2(Q^2 = 0) - \frac{N_C}{16\pi^2} \frac{4}{3} g_A^2 \Gamma(1, \epsilon) \quad (115)$$

3.3 The Scalar Two-Point Function

The full scalar invariant function from the sum of the infinite series of bubble diagrams has the form

$$\Pi_S(Q^2) = \frac{\bar{\Pi}_S(Q^2)}{1 - \frac{4\pi^2 G_S}{N_C \Lambda_\chi^2} \bar{\Pi}_S(Q^2)}. \quad (116)$$

It only involves the four-quark operator with G_S -coupling. As in the previous vector and axial-vector discussion, we now proceed to the calculation of the scalar two-point function $\bar{\Pi}_S(Q^2)$ in the mean field approximation. The associated spectral function can be calculated unambiguously, with the result

$$\frac{1}{\pi} \text{Im} \bar{\Pi}_S(t) = \frac{N_C}{16\pi^2} 8M_Q^2 \left(\frac{t}{4M_Q^2} - 1 \right) \sqrt{1 - \frac{4M_Q^2}{t}} \theta(t - 4M_Q^2). \quad (117)$$

From its asymptotic behaviour at large t , it follows that the function $\bar{\Pi}_S(Q^2)$ obeys a dispersion relation with two-subtractions for the term proportional to $t\sqrt{1 - 4M_Q^2/t}$ and one subtraction for the term $M_Q^2\sqrt{1 - 4M_Q^2/t}$. Accordingly, we write the dispersion relation

$$\begin{aligned} \bar{\Pi}_S(Q^2) &= \bar{\Pi}_S(0) + Q^2 \left(\bar{\Pi}'_S(0) - \frac{N_C}{16\pi^2} \frac{4}{3} \Gamma(1, \epsilon) \right) \\ &- Q^2 \int_0^\infty \frac{dt}{t} \frac{1}{t + Q^2} \frac{N_C}{16\pi^2} (-8M_Q^2) \sqrt{1 - \frac{4M_Q^2}{t}} \theta(t - 4M_Q^2) \\ &+ Q^4 \int_0^\infty \frac{dt}{t^2} \frac{1}{t + Q^2} \frac{N_C}{16\pi^2} (2t) \sqrt{1 - \frac{4M_Q^2}{t}} \theta(t - 4M_Q^2); \end{aligned} \quad (118)$$

where $\bar{\Pi}_S(0)$ and $\bar{\Pi}'_S(0)$ are already known from the effective action calculation i.e.,

$$\bar{\Pi}_S(0) = \frac{N_C}{16\pi^2} 4M_Q^2 [\Gamma(-1, \epsilon) - 2\Gamma(0, \epsilon)]; \quad (119)$$

and

$$\overline{\Pi}_S(0) = -\frac{N_C}{16\pi^2} 2 \left(\Gamma(0, \epsilon) - \frac{2}{3} \Gamma(1, \epsilon) \right) . \quad (120)$$

Notice that only the divergent pieces (i.e., terms proportional to $\Gamma(-1, \epsilon)$ and $\Gamma(0, \epsilon)$; but not $\Gamma(n, \epsilon)$, $n \simeq 1$) are retained in the subtraction constant. The integral we have to compute is

$$\int_{4M_Q^2}^{\infty} \frac{dt}{t} \frac{1}{t+Q^2} \sqrt{1 - \frac{4M_Q^2}{t}} = \frac{1}{2} \int_0^1 dx (1-2x)^2 \frac{1}{M_Q^2 + Q^2 x(1-x)} , \quad (121)$$

where we have made the standard change of variables of eq. (73). Using the representation of eq. (75), and doing one integration by parts in the variable x , and replacing eqs. (119) and (120), we obtain the result ($\epsilon = \frac{M_Q^2}{\Lambda_\chi^2}$, $x_Q = \frac{M_Q^2 + Q^2 x(1-x)}{\Lambda_\chi^2}$)

$$\overline{\Pi}_S(Q^2) = \frac{N_C}{16\pi^2} 4M_Q^2 \left\{ \Gamma(-1, \epsilon) - 2 \left(\frac{Q^2}{4M_Q^2} + 1 \right) \int_0^1 dx \Gamma(0, x_Q) \right\} . \quad (122)$$

We shall next evaluate the full $\Pi_S(Q^2)$ function in eq. (116), and try to cast it in a form as close as possible to eq. (54):

$$\Pi_S(Q^2) = \frac{\frac{N_C \Lambda_\chi^2}{4\pi^2 G_S} \overline{\Pi}_S(Q^2)}{\frac{N_C \Lambda_\chi^2}{4\pi^2 G_S} - \overline{\Pi}_S(Q^2)} . \quad (123)$$

Using the fact that $G_S^{-1} = \epsilon \Gamma(-1, \epsilon)$, we can cancel the terms proportional to $\Gamma(-1, \epsilon)$ in the denominator; and write $\Pi_S(Q^2)$ in the simple form

$$\Pi_S(Q^2) = 8B_0^2 \left\{ 2\tilde{L}_8 + \tilde{H}_2 + \frac{2c_m^2(Q^2)}{Q^2 + M_S^2} \right\} , \quad (124)$$

where

$$M_S^2 = 4M_Q^2 , \quad (125)$$

and ($x_Q = \frac{M_Q^2 + Q^2 x(1-x)}{\Lambda_\chi^2}$)

$$8B_0^2 \times \frac{2c_m^2(Q^2)}{M_S^2} = \frac{N_C}{16\pi^2} 4M_Q^2 \frac{(\Gamma(-1, \epsilon))^2}{2 \int_0^1 dx \Gamma(0, x_Q)} = \frac{\langle \bar{Q}Q \rangle^2}{2M_Q^2 f_\pi^2(Q^2)} . \quad (126)$$

The term

$$8B_0^2 (2\tilde{L}_8 + \tilde{H}_2) = -\frac{N_C}{16\pi^2} 4M_Q^2 \Gamma(-1, \epsilon) = \frac{\langle \bar{Q}Q \rangle}{M_Q} \quad (127)$$

is not quite the same as in the effective action calculation. The value of $\Pi_S(Q^2 = 0)$ however, coincides with the same result as in the effective action:

$$\Pi_S(0) = 8B_0^2 (2L_8 + H_2) = \frac{N_C}{16\pi^2} 4M_Q^2 \frac{\Gamma(-1, \epsilon)}{2\Gamma(0, \epsilon)} [\Gamma(-1, \epsilon) - 2\Gamma(0, \epsilon)] . \quad (128)$$

As in the previous subsection, it was an advantage to reabsorb some of the constant terms into the pole term, compared with the expression obtained from the effective action calculation, to obtain a simple expression to all orders in Q^2 .

The striking new feature of the summed scalar propagator is that the scalar mass is constant and $M_S = 2M_Q$. This is to be contrasted with results of previous work in the literature, see e.g. ref. [21] and references therein. Eqs. (125) and (127) are also true in the presence of gluonic corrections. They, and the fact that $M_S = 2M_Q$, are a consequence of the identities derived in the appendix. It is only the specific form of the functions that depends on the inclusion of gluons or not.

3.4 Two-Point Functions with Mixing

The case of the other two-point functions $\Pi_A^{(0)}(Q^2)$, $\Pi_M^P(Q^2)$ and $\Pi^P(Q^2)$ is somewhat more involved because they mix through the Nambu–Jona-Lasinio four-fermion interaction terms in eqs. (34) and (35). Therefore, for this case the result at the n bubble level is a matrix equation in terms of the two-point functions at the $n-1$ bubble level:

$${}^n\Pi \equiv \begin{pmatrix} {}^n\Pi_A^{(0)} \\ {}^n\Pi_M^P \\ {}^n\Pi_P \end{pmatrix} = \begin{pmatrix} g_V \bar{\Pi}_A^{(0)} & g_S \bar{\Pi}_M^P & 0 \\ 0 & g_V \bar{\Pi}_A^{(0)} & g_S \bar{\Pi}_M^P \\ 0 & g_V \bar{\Pi}_M^P & g_S \bar{\Pi}_P \end{pmatrix} \times \begin{pmatrix} {}^{n-1}\Pi_A^{(0)} \\ {}^{n-1}\Pi_M^P \\ {}^{n-1}\Pi_P \end{pmatrix}, \quad (129)$$

where $\bar{\Pi}_V^{(0)}(Q^2)$, $\bar{\Pi}_M^P(Q^2)$ and $\bar{\Pi}_P(Q^2)$ denote, as usual the two-point functions at the one loop level calculated in the mean field approximation; and g_V , g_S are short-hand notation for

$$g_V = \frac{8\pi^2 G_V}{N_C \Lambda_\chi^2} Q^2 \quad \text{and} \quad g_S = \frac{4\pi^2 G_S}{N_C \Lambda_\chi^2}. \quad (130)$$

The series we have to sum, in a vector-like notation, is

$$\Pi(Q^2) = \sum_{n=1}^{\infty} {}^n\Pi = \sum_{n=1}^{\infty} B^{n-1}(Q^2) \bar{\Pi}(Q^2), \quad (131)$$

where $B(Q^2)$ denotes the 3×3 two-point function matrix in eq. (129); and the $\Pi(Q^2)$'s three component two-point function vectors. This series can be summed,

$$\Pi(Q^2) = \frac{1}{1 - B(Q^2)} \bar{\Pi}(Q^2). \quad (132)$$

The matrix $(1 - B)$ can be inverted, and after some algebra we get the result

$$\Pi_A^{(0)}(Q^2) = \frac{1}{\Delta(Q^2)} \left[(1 - g_S \bar{\Pi}^P) \bar{\Pi}_A^{(0)} + g_S (\bar{\Pi}_M^P)^2 \right]; \quad (133)$$

$$\Pi_M^P(Q^2) = \frac{1}{\Delta(Q^2)} \bar{\Pi}_M^P(Q^2); \quad (134)$$

and

$$\Pi_P(Q^2) = \frac{1}{\Delta(Q^2)} \left[(1 - g_V \bar{\Pi}_A^{(0)}) \bar{\Pi}_P + g_V (\bar{\Pi}_M^P)^2 \right], \quad (135)$$

with $\Delta(Q^2)$ the function

$$\Delta(Q^2) = \left(1 - g_V \bar{\Pi}_A^{(0)} \right) \left(1 - g_S \bar{\Pi}_P \right) - g_S g_V (\bar{\Pi}_M^P)^2. \quad (136)$$

It is illustrative to see what the result would be for the scalar two-point function $\Pi^S(Q^2)$ if we had carried the analysis keeping the functions $\bar{\Pi}_V^{(0)}$ and $\bar{\Pi}_M^S$:

$$\Pi_S(Q^2) = \frac{-g_V (\bar{\Pi}_M^S)^2 + (1 - g_V \bar{\Pi}_V^{(0)}) \bar{\Pi}_S}{(1 - g_V \bar{\Pi}_V^{(0)}) (1 - g_S \bar{\Pi}_S) + g_S g_V (\bar{\Pi}_M^S)^2}. \quad (137)$$

If we now set $\bar{\Pi}_V^{(0)} = \bar{\Pi}_M^S = 0$, we recover the result of eq. (116).

We need now to calculate $\bar{\Pi}_P(Q^2)$ and $\bar{\Pi}_M^P(Q^2)$. To calculate $\bar{\Pi}_P(Q^2)$ we proceed as for the other two-point functions we have already calculated. The corresponding spectral function is

$$\frac{1}{\pi} \text{Im} \bar{\Pi}_P(t) = \frac{N_C}{16\pi^2} 8M_Q^2 \frac{t}{4M_Q^2} \sqrt{1 - \frac{4M_Q^2}{t}} \theta(t - 4M_Q^2). \quad (138)$$

For the large t -behaviour we conclude that $\bar{\Pi}_P(Q^2)$ obeys a dispersion relation subtracted twice:

$$\bar{\Pi}_P(Q^2) = \bar{\Pi}_P(0) + Q^2 \bar{\Pi}'_P(0) + Q^4 \int_0^\infty \frac{dt}{t^2} \frac{1}{t + Q^2} \frac{1}{\pi} \text{Im} \bar{\Pi}_P(t), \quad (139)$$

with the divergent pieces (divergent when $\epsilon = M_Q^2/\Lambda_\chi^2 \rightarrow 0$) of $\bar{\Pi}_P(0)$ and $\bar{\Pi}'_P(0)$ as known from the effective action calculation i.e.,

$$\bar{\Pi}_P(0) = \frac{N_C}{16\pi^2} 4M_Q^2 \Gamma(-1, \epsilon); \quad (140)$$

and

$$\bar{\Pi}'_P(0) = -\frac{N_C}{16\pi^2} 2\Gamma(0, \epsilon). \quad (141)$$

The integral in the r.h.s. of eq. (139) has already been calculated in the section about the scalar two-point function. We then find the result ($x_Q = \frac{M_Q^2 + Q^2 x(1-x)}{\Lambda_\chi^2}$)

$$\bar{\Pi}_P(Q^2) = \frac{N_C}{16\pi^2} \left\{ 4M_Q^2 \Gamma(-1, \epsilon) - 2Q^2 \int_0^1 dx \Gamma(0, x_Q) \right\}. \quad (142)$$

Let us check that this result satisfies the three criteria we discussed in section 3.1. First, there is a Ward identity which relates $\bar{\Pi}_P(Q^2)$ to $\bar{\Pi}_A^{(0)}(Q^2)$, because of the axial current divergence condition

$$\partial_\mu (\bar{Q} \gamma^\mu \gamma_5 Q) = 2M_Q \bar{Q} i \gamma_5 Q \quad (143)$$

in the mean effective field theory. The Ward identity in question, which we proof in the appendix, is

$$4M_Q^2 \bar{\Pi}_P(Q^2) + 4M_Q \langle \bar{Q}Q \rangle = (Q^2)^2 \bar{\Pi}_A^{(0)}(Q^2) ; \quad (144)$$

and [13]

$$\langle \bar{Q}Q \rangle = -\frac{N_C}{16\pi^2} 4M_Q^3 \Gamma(-1, \epsilon) . \quad (145)$$

Equations (97) and (142) indeed satisfy this Ward identity. Second, the spectral function calculated from eq. (142) via the $i\epsilon$ prescription:

$$\log \frac{M_Q^2 - tx(1-x) - i\epsilon}{\Lambda_\chi^2} = \log \left| \frac{M_Q^2 - tx(1-x)}{\Lambda_\chi^2} \right| + i\pi \theta \left(\frac{tx(1-x) - M_Q^2}{\Lambda_\chi^2} \right) ,$$

is the same as in eq. (138). Finally, the first few terms in the Q^2 -expansion of $\Pi_P(Q^2)$ coincide with those calculated in the effective action approach with the proper time heat kernel regularization.

The last two-point function to calculate is $\Pi_M^P(Q^2)$. The corresponding spectral function is

$$\frac{1}{\pi} \text{Im} \bar{\Pi}_M^P(t) = \frac{N_C}{16\pi^2} 4M_Q \sqrt{1 - \frac{4M_Q^2}{t}} \theta(t - 4M_Q^2) . \quad (146)$$

The function $\bar{\Pi}_M^P(Q^2)$ obeys a once subtracted dispersion relation. We already have encountered the same situation with one of the terms in the scalar two-point function, which we have discussed in detail. Therefore, we give the final result only

$$\bar{\Pi}_M^P(Q^2) = \frac{N_C}{16\pi^2} 4M_Q \int_0^1 dx \Gamma(0, x_Q) . \quad (147)$$

We can now proceed to the explicit calculation of the functions $\Pi_A^{(0)}(Q^2)$, $\Pi_M^P(Q^2)$ and $\Pi_P(Q^2)$ in eqs. (133), (134) and (135). We find that

$$\left[1 - g_S \bar{\Pi}_P(Q^2) \right] \bar{\Pi}_A^{(0)}(Q^2) + g_S \left(\bar{\Pi}_M^P(Q^2) \right)^2 = 0 , \quad (148)$$

and hence

$$\Pi_A^{(0)}(Q^2) = 0 , \quad (149)$$

a result which must hold in QCD at the chiral limit. Equation (148) also implies that

$$\Delta(Q^2) = 1 - g_S \bar{\Pi}_P(Q^2) = \frac{Q^2}{M_Q^2} \frac{1}{2\Gamma(-1, \epsilon)} \int_0^1 dx \Gamma(0, x_Q) ; \quad (150)$$

and therefore

$$\Pi_M^P(Q^2) = -2 \frac{\langle \bar{Q}Q \rangle}{Q^2} . \quad (151)$$

As for $\Pi_P(Q^2)$, from eq. (135) and using the relations (148) and (150) above, we find

$$\Pi_P(Q^2) = \frac{\overline{\Pi}_P(Q^2) - g_V/g_S \overline{\Pi}_A^{(0)}(Q^2)}{1 - g_S \overline{\Pi}_P(Q^2)} = \frac{\langle \bar{Q}Q \rangle}{M_Q} + \frac{2\langle \bar{Q}Q \rangle^2}{f_\pi^2(Q^2) Q^2} . \quad (152)$$

We see from this result that mixing between the pseudoscalar and the longitudinal axial degrees of freedom occurs at all orders in the Q^2 -expansion. Because of eq. (150), $\Pi_P(Q^2)$ has now a pole at $Q^2 = 0$. We want to stress the fact that the final full results in eqs. (149), (151) and (152) are very different to those at the one-loop level approximation. It is only when all the contribution to leading order in $1/N_C$ are summed that these relations, which are expected features of QCD, appear. These results are a big improvement with respect to the QCD effective action approach at the mean field approximation.

3.5 Inclusion of Gluonic Corrections

In Ref. [13] the low-energy corrections due to the lowest dimensional gluonic condensate were also explicitly included. A general analysis based on the possible types of terms here corresponds essentially to keeping all the overlined functions as undetermined parameters but satisfying the relations derived in the appendix. This follows from the fact that gluonic lines connecting different fermion loops in Fig. 2a are suppressed by extra factors of $1/N_c$ compared to the leading contribution.

The correction due to the leading gluonic vacuum expectation values can in fact be easily included by using the results for two-point functions calculated for use in QCD sum rules [9]. These corrections can be rewritten in terms of the dimensionless parameter

$$g = \frac{\pi^2}{6N_c m_Q^4} \langle \frac{\alpha_s}{\pi} G^2 \rangle \quad (153)$$

and the set of functions

$$\mathcal{J}_N = \int_0^1 dx \frac{1}{\left(1 + \frac{Q^2}{m_Q^2} x(1-x)\right)^N} . \quad (154)$$

The corrections needed for the spin-1 parts are (for $N_c = 3$)

$$\begin{aligned} \overline{\Pi}_V^{(1)}(Q^2) &= \frac{3gM_Q^4}{2\pi^2 Q^4} (-1 + 3\mathcal{J}_2 - 2\mathcal{J}_3) , \\ \overline{\Pi}_A^{(1)}(Q^2) &= \frac{9gM_Q^4}{2\pi^2 Q^4} (1 - \mathcal{J}_2) . \end{aligned} \quad (155)$$

For the scalar two-point function we need

$$\overline{\Pi}_S(Q^2) = \frac{9gM_Q^4}{4\pi^2 Q^4} (-1 - 2\mathcal{J}_1 + 3\mathcal{J}_2) . \quad (156)$$

The spin-0 axial-vector, pseudo-scalar and mixed two-point functions have very large cancellations in the denominator and are numerically very unstable when gluonic corrections are included. They can be handled similarly in principle. The gluonic correction terms do also satisfy the relations derived in the appendix as required.

We have checked that using the above formulas the two-point functions including non-zero gluonic vacuum expectation values converge for small values of Q^2 to the low energy expansion with these corrections included; i.e. those of eqs. (21)-(28) with the values of the parameters calculated including gluonic corrections. All the nice features of the two-point functions as given in the previous subsections are still valid since the underlying cause for these properties were the relations derived in the appendix and the gluonic corrections have to satisfy those as well.

3.6 Numerical Results

In this section we plot the two-point functions as calculated in the previous subsections. As described in subsection 3.5 we can also include gluonic corrections. In view of the result of ref. [13] that a very good fit to the low-energy parameters could also be obtained without gluonic corrections, we only show the effect of the gluonic corrections in the vector two-point functions. The input values used for all of the plots are those of fit 1 in ref. [13]. They are $M_Q = 0.265 \text{ GeV}$, $\Lambda_\chi = 1.165 \text{ GeV}$ and $g_A = 0.61$. The variation with the input parameters can be judged from table 2 in ref. [13]. The size of the changes here is similar to the ones obtained there at values of momentum transfer $Q^2 = 0$.

In fig. 4 we have plotted the vector-two-point function for positive values of Q^2 for $\sqrt{Q^2}$ from 0 to 1.5 GeV . The full line corresponds to $\bar{\Pi}_V^{(1)}(q^2)$ in the full ENJL-model. The dashed line is the corresponding result using the effective approximation, eq. (56). The vector meson mass for the values of the parameters M_Q , Λ_χ and g_A which we have fixed, is about 0.81 GeV . The short-dashed line corresponds to the vector-two-point function in the QCD effective action model of ref. [15]. As can be seen in the figure, the full resummation leads to lower values for the two point functions than those of the low-energy formulas when extended to higher Q^2 . In the same figure 4 we also show the effect of the gluonic corrections. The dotted line uses the same input values as given above but has a non-zero value for the gluonic background, we have set $g = 0.5$ (see eq. (153)). It can be seen that the effect of gluonic corrections is large at small values of Q^2 but grows smaller at higher values of Q^2 .

In fig. 5 we have plotted similarly to the vector case, the result for $Q^2\Pi_1^A(Q^2)$. (The extra factor of Q^2 is included to remove the pole at $Q^2 = 0$ due to pion exchange.) In contrast to the vector two-point function, there is also a significant

difference between the one-loop result of eq. (57) (dashed line) and the full resummation of eq. (105) at low Q^2 (the full line). This is due to what is usually called the pseudoscalar-axial-vector mixing and was in our previous work described by the coupling g_A . The value of this two-point function at $Q^2 = 0$ determines f_π^2 . The dashed line corresponds to the two-point function using the effective approximation of eq. (57). The axial-vector mass here is about 1.3 GeV .

Fig. 6 shows how the summation of the whole series of diagrams has produced the pole at $Q^2 = 0$ that is required by the spontaneous breaking of the chiral symmetry for the pseudoscalar two-point function. The one-loop result (dashed line) does not have this behaviour, but the full resummed version (full line) of eq. (152) does. The short-dashed line is the low-energy extrapolation of eq. (28). Here we see how the full resummation correctly reproduces the low-energy behaviour as derived in ref. [13], but for larger values of momentum transfer, it starts to differ appreciably.

We have not plotted the scalar two-point function. The pole is, as we have proven above, always at $M_S = 2M_Q$. This pole is generated by the full resummation. Neither have we plotted the mixed pseudoscalar-axial-vector two-point function since this has the very simple behaviour of Eq. (151).

The overall picture of the high energy behaviour of the ENJL-model that emerges after the resummation, is improved compared to the behaviour obtained from the low-energy expansion. This is illustrated by the fact that now it also satisfies the second Weinberg sum rule. The ENJL-model has another advantage over the simple QCD effective action model of ref. [15]. By virtue of the extra 4-quark interactions present, this model naturally contains more or less correct meson poles while the simple quark version, that corresponds to the one-loop result (or essentially the use of the overlined two-point functions), does not. This means that for positive values of q^2 the two-point functions are considerably enhanced both in the real and imaginary parts as compared to the one loop result. The importance of this type of behaviour can be seen, e.g. in the determination of some low-energy constants using dispersion relations. As an example we show in fig. 3 how the imaginary part of the vector two-point function gets enhanced considerably over the one-loop result.

The advantage of using the full ENJL-model over a parametrization with meson resonances is that the number of free parameters remains within limits. For instance, if one tries to extend the analysis of ref. [16] to non-leptonic matrix elements using a parametrization with vector mesons it requires the knowledge of weak decays of vector mesons which have not been observed experimentally.

In ref. [13] the masses and couplings of the mesons were determined from the low-energy expansion. These are essentially given by various combinations of derivatives of the two-point functions at $q^2 = 0$. An alternative way of determining the meson

masses is to determine them by looking for the poles and residues of the full two-point functions. This procedure can be questioned on the grounds that for euclidean momenta quark confinement is not so important but for momenta of $q^2 \geq 4M_Q^2$ we get effects of free quarks included. The two-point functions still have poles though. As an example we give the position of the poles for the vector, axial-vector and scalar for the parameters used above, in table 1. The pion mass is of course exactly zero in both cases since we work in the chiral limit. In general the masses are lower than those derived from the low energy approximation.

4 THE $\pi^+-\pi^0$ ELECTROMAGNETIC MASS DIFFERENCE

To the lowest order in the chiral expansion, the effect of virtual electromagnetic interactions to lowest order in the fine structure constant $\alpha_{em} = e^2/4\pi$, generates a term in the effective action without derivatives [22]:

$$\int d^4x \left\{ e^2 C_1 \text{tr} Q U(x) Q U^+(x) \right\} , \quad (157)$$

where U is the unitary matrix which collects the pseudoscalar Goldstone fields and Q the quark electric charge matrix $Q = 1/3 \text{diag}(2, -1, -1)$. Expanding eq. (157) in powers of pseudoscalar fields

$$e^2 C_1 \text{tr} Q U Q U^+ = -\frac{2e^2 C_1}{f_\pi^2} (\pi^+ \pi^- + K^+ K^-) + \mathcal{O}(\phi^4) , \quad (158)$$

one sees explicitly that this term leads to a $\pi^+-\pi^0$ (and K^+-K^0) mass splitting

$$\Delta m_\pi^2 = \left(m_{\pi^+}^2 - m_{\pi^0}^2 \right)_{EM} = \frac{2e^2 C_1}{f_\pi^2} . \quad (159)$$

The constant C_1 , like f_π^2 , is not fixed by symmetry requirement alone. It is determined by the dynamics of the underlying theory. Formally, it is given by the integral representation [14]

$$2e^2 C_1 = -ie^2 \int \frac{d^4q}{(2\pi)^4} \frac{g_{\mu\nu} - \frac{q_\mu q_\nu}{q^2}}{q^2 - i\epsilon} (q^\mu q^\nu - q^2 g^{\mu\nu}) \Pi_{LR}^{(1)}(q^2) , \quad (160)$$

where

$$\Pi_{LR}^{(1)} = \frac{1}{2} \left(\Pi_V^{(1)} - \Pi_A^{(1)} \right) , \quad (161)$$

with $\Pi_V^{(1)}$ and $\Pi_A^{(1)}$ the vector and axial vector invariant functions we have discussed. Performing a Wick rotation in eq. (160) leads to the sum rule [2]

$$\Delta m_\pi^2 = \frac{\alpha_{em}}{\pi} \frac{1}{16\pi^2 f_\pi^2} (-6\pi^2) \int_0^\infty \frac{dQ^2}{Q^2} Q^4 \left[\Pi_V^{(1)}(Q^2) - \Pi_A^{(1)}(Q^2) \right] . \quad (162)$$

The purpose of this section is to discuss the evaluation of the Δm_π^2 sum rule above based on the two-point function results discussed in the previous sections. It is then convenient to split the Q^2 -integral into long-distance ($0 \leq Q^2 \leq \mu^2$) and short-distance ($\mu^2 \leq Q^2 \leq \infty$) parts:

$$\int_0^\infty dQ^2 \dots = \int_0^{\mu^2} dQ^2 \dots + \int_{\mu^2}^\infty dQ^2 \dots \quad (163)$$

We shall concentrate first on the long-distance part calculation.

a) Long-distance contribution. Phenomenological approach

The very low Q^2 contribution to the integral

$$\left(\Delta m_\pi^2\right)_{LD} = \frac{\alpha_{em}}{\pi} \left(\frac{-3}{8f_\pi^2}\right) \int_0^{\mu^2} dQ^2 Q^2 \left(\Pi_V^{(1)} - \Pi_A^{(1)}\right) \quad (164)$$

is fixed by chiral perturbation theory (see eqs. (21) and (23)):

$$\Pi_V^{(1)}(Q^2) - \Pi_A^{(1)}(Q^2) = \frac{-2f_\pi^2}{Q^2} - 8L_{10} + \mathcal{O}(Q^2), \quad (165)$$

from which it follows that [14]

$$\left(\Delta m_\pi^2\right)_{\chi PT} = \frac{\alpha_{em}}{\pi} \frac{3}{4} \mu^2 \left\{ 1 + \frac{2L_{10}}{f_\pi^2} \mu^2 + \mathcal{O}(\mu^4) \right\}. \quad (166)$$

The known correction term $\mathcal{O}(\mu^2)$ in the parenthesis of the r.h.s. can be used to estimate the value of the μ^2 -scale at which we can trust the validity of the χ PT-contribution. From the fact that [20]

$$\frac{4L_{10}}{f_\pi^2} \simeq -\frac{1}{M_\rho^2}, \quad (167)$$

we conclude that the χ PT-result in eq. (166) can only represent correctly the long-distance contribution to Δm_π^2 up to scales

$$\mu_{\chi PT}^2 < M_\rho^2. \quad (168)$$

Obviously, this is too small a scale to trust numerically a direct matching with the short-distance contribution, which as we shall see later, it is expected to be valid for μ^2 -scales larger than a few GeV^2 at least. (See however the first paper in ref.[22] and ref. [14].)

Since the early work of Das et. al. [2], the traditional phenomenological approach to the calculation of $\left(\Delta m_\pi^2\right)_{LD}$ has been to include the effect of vector and axial-vector particle states in the Q^2 -integral, using a parametrization that is constrained

to satisfy the first and second Weinberg sum rules. The usual phenomenological VMD-model parametrization is

$$\Pi_V^{(1)} = \frac{2f_V^2 M_V^2}{M_V^2 + Q^2} \quad (169)$$

and

$$\Pi_A^{(1)} = \frac{2f_\pi^2}{Q^2} + \frac{2f_A^2 M_A^2}{M_A^2 + Q^2} , \quad (170)$$

with the constants f_π^2 , f_V^2 , f_A^2 , M_V^2 and M_A^2 constrained by the relations

$$f_\pi^2 + f_A^2 M_A^2 = f_V^2 M_V^2 \quad (171)$$

and

$$f_V^2 M_V^4 = f_A^2 M_A^4 , \quad (172)$$

which ensure the convergence of the limits

$$\lim_{Q^2 \rightarrow \infty} Q^2 (\Pi_V^{(1)} - \Pi_A^{(1)}) \rightarrow 0 \quad \text{and} \quad \lim_{Q^2 \rightarrow \infty} Q^4 (\Pi_V^{(1)} - \Pi_A^{(1)}) \rightarrow 0 ; \quad (173)$$

i.e., the superconvergence relations which lead to the first and second Weinberg sum rules. One then has

$$\left(\Delta m_\pi^2 \right)_{VMD} = \frac{\alpha_{em}}{\pi} \frac{3}{4} \int_0^{\mu^2} dQ^2 \frac{M_A^2 M_V^2}{(Q^2 + M_A^2)(Q^2 + M_V^2)} \quad (174)$$

For $M_A, M_V \rightarrow \infty$, with μ^2 fixed we recover the first term of the χ PT calculation in eq. (166). If we let the scale μ^2 go to infinity; then, for $M_A = \sqrt{2}M_V$, one finds the early result of Das et al. :

$$\left(\Delta m_\pi^2 \right)_{[2]} = \frac{\alpha_{em}}{\pi} \frac{3}{2} M_\rho^2 \log 2 = 1.4 \times 10^3 MeV^2 . \quad (175)$$

Experimentally,

$$(m_{\pi^+} - m_{\pi^0})_{Exp.} = (4.5936 \pm 0.0005) MeV , \quad (176)$$

while the phenomenological result of Das et al. corresponds to

$$(m_{\pi^+} - m_{\pi^0})_{[2]} = 5.2 MeV , \quad (177)$$

Recent phenomenological evaluations of the Δm_π^2 sum rule, which include explicit chiral symmetry breaking effects, can be found in refs.[23] to [25].

b) Long-distance contribution in the ENJL-model

The calculation of $(\Delta m_\pi^2)_{LD}$ in the QCD effective action approach of ref. [15], which corresponds to the mean field approximation of the Nambu Jona-Lasinio model, was reported in ref.[14]. It is the approximation where

$$\Pi_V^{(1)} - \Pi_A^{(1)} \rightarrow \bar{\Pi}_V^{(1)} - \bar{\Pi}_A^{(1)} = -\frac{N_C}{16\pi^2} \frac{8M_Q^2}{Q^2} \int_0^1 dx \Gamma(0, xQ) , \quad (178)$$

which is the result obtained in eqs. (92) and (97). This leads to the result ($\epsilon = M_Q^2/\Lambda_\chi^2, x_Q = \frac{Q^2 x(1-x)+M_Q^2}{\Lambda_\chi^2}$)

$$(\Delta m_\pi^2)_{[14]} = \frac{\alpha_{em}}{\pi} \frac{3}{4} \int_0^{\mu^2} dQ^2 \frac{1}{\Gamma(0, \epsilon)} \int_0^1 dx \Gamma(0, x_Q) . \quad (179)$$

In ref.[14] a proper time regularization for the photon propagator was used; and for simplicity, the μ^2 -scale was identified with Λ_χ^2 . The shape of this mean field approximation evaluation versus μ^2 , for the input value of M_Q^2 and Λ_χ^2 which we have been considering (i.e., the value corresponding to fit 1 in ref.[13]: $M_Q = 265 MeV$ and $\Lambda_\chi = 1165 MeV$) is plotted in Fig. 7.

The evaluation of $(\Delta m_\pi^2)_{LD}$ in the full ENJL-model, with the expressions of the two-point functions $\Pi_V^{(1)}(Q^2)$ and $\Pi_A^{(1)}(Q^2)$ obtained in the previous section leads to the result

$$(\Delta m_\pi^2)_{ENJL} = \frac{\alpha_{em}}{\pi} \frac{3}{4} \int_0^{\mu^2} dQ^2 \frac{f_\pi^2(Q^2)}{f_\pi^2} \frac{M_A^2(Q^2) M_V^2(Q^2)}{(Q^2 + M_A^2(Q^2))(Q^2 + M_V^2(Q^2))} , \quad (180)$$

with the Q^2 -dependent functions $M_V^2(Q^2)$, $M_A^2(Q^2)$ and $f_\pi^2(Q^2)$ as given by eqs. (82), (107), (104) and (106).

The shape of $(\Delta m_\pi^2)_{ENJL}$ versus μ^2 is shown in Fig. 7. We expect the integrand in eq. (180) to be a good representation of the low and intermediate energy scales; and therefore, the matching with short-distance evaluation should now be much smoother than in the case of the mean field approximation. This we discuss in the next subsection.

c) Short-distance contribution and numerical results.

In QCD perturbation theory $\Pi_V^{(1)}(Q^2) = \Pi_A^{(1)}(Q^2)$. Spontaneous symmetry breaking induces a deviation from this result which, at large Q^2 and to leading order in the $1/N_C$ -expansion, can be calculated using the operator product expansion, with the result ([8] and first ref. in [22])

$$(\Pi_V^{(1)} - \Pi_A^{(1)}) = -\frac{1}{Q^6} \frac{3\pi^2}{2} \frac{N_C \alpha_s(Q^2)}{\pi} (\langle \bar{\psi}\psi \rangle)^2 , \quad (181)$$

where ($N_C \rightarrow \infty$):

$$\frac{N_C \alpha_s(Q^2)}{\pi} \rightarrow \frac{6}{11 \log(\frac{Q}{\Lambda_{QCD}})} ; \quad (182)$$

and

$$\langle \bar{\psi}\psi(Q^2) \rangle = \langle \hat{\psi}\psi \rangle (\log(Q/\Lambda_{QCD}))^{\frac{9}{22}} . \quad (183)$$

Inserting this asymptotic estimate in the short-distance expression for Δm_π^2 , leads to the result

$$(\Delta m_\pi^2)_{SD} = \frac{\alpha_{em}}{\pi} \frac{27\pi^2}{88 f_\pi^2} \left(\frac{\langle \hat{\psi}\psi \rangle}{\mu^2} \right)^2 \int_1^\infty \frac{dz}{z^2} \left(\frac{1}{2} \log \left(\frac{\mu^2}{\Lambda_{QCD}^2} z \right) \right)^{-\frac{2}{11}} . \quad (184)$$

Fig.7 also shows the shape of $(\Delta m_\pi^2)_{SD}$ versus μ^2 for various values of the invariant quark condensate $\langle \hat{\psi}\psi \rangle$. * Obviously, as the scale μ^2 becomes small $(\Delta m_\pi^2)_{SD}$ diverges. The matching between $(\Delta m_\pi^2)_{SD}$ and $(\Delta m_\pi^2)_{LD}$ is defined by the optimal choice of μ^2 which minimizes the variation of the total Δm_π^2 . As seen in fig. 8 this occurs at value $\mu \approx 950 \text{ MeV}$; and in fact around the value, the stability is rather good. The corresponding value of Δm_π^2 in this range, is

$$\Delta m_\pi^2 \approx 1.3 \cdot 10^{-3} \text{ GeV}^2, \quad (185)$$

and agree well with the experimental value, the horizontal dashed line in fig. 8.

5 CONCLUSIONS

In this paper we have extended the general analysis of the ENJL-model as done in ref. [13] beyond the low-energy expansion. We have calculated directly the two-point functions within the ENJL-model to all orders in momenta. The relations that the one-loop results have to satisfy lead after the full resummation to a set of rather simple forms for the two-point functions. It should be stressed once more that these are satisfied independent of the gluonic interactions and are thus valid in a wide class of ENJL-like models.

The resulting expressions are, for the vector-axial-vector cases, very similar to the ones usually obtained assuming some kind of vector, axial-vector meson dominance. The full resummations have a well behaved high-energy behaviour. They satisfy both the first and the second Weinberg sum rules. The resummation also obeys the Ward identities of the full theory.

Simple expressions were also found for the other two-point functions. A byproduct was a proof that within this class of models the scalar two-point function always has a pole corresponding to a mass of twice the constituent quark mass. Our derivation only depends on the underlying symmetry properties of the Lagrangian and is hence regularization scheme independent. The full resummation also reproduced the pole at $Q^2 = 0$ in the pseudo-scalar two-point function explicitly showing how this model obeys the Goldstone theorem.

Finally, the two-point functions derived were used to start evaluating nonleptonic matrix elements within the class of ENJL-like models. We have estimated the electromagnetic $\pi^+ - \pi^0$ mass difference and found good agreement with the measured value.

*The continuous curve is the one corresponding to the choice $|\langle \bar{\psi}\psi \rangle| = (281 \text{ MeV})^3$, which is the value predicted in the ENJL-model for the input values $M_Q = 265 \text{ MeV}$ and $\Lambda_\chi = 1162 \text{ MeV}$.

ACKNOWLEDGEMENTS

We would like to thank Ch. Bruno for collaboration in the early stages of this work and helpful comments. H.Z. would like to thank the ICSC world laboratory for financial support. J.B. thanks CPT Marseille for hospitality.

APPENDIX

In this appendix we derive the Ward identities that the one-loop two-point functions have to satisfy. We first give a derivation based on the heat-kernel expansion and a general analysis of the type of terms that can contribute to the two-point functions. This method allows for explicit contact to be made with the regularization chosen in the heat-kernel expansion. A second method is essentially the traditional way of deriving Ward identities but we have to take into account that $\langle \bar{q}q \rangle \neq 0$. The second method can also be used to derive some of the identities that the full two-point functions have to satisfy.

The one-loop two-point functions are calculated using the Lagrangian ($U = 1$)

$$\mathcal{L} = \bar{q}i\mathcal{D}q - M_Q\bar{q}q - \bar{q}(s - ip\gamma_5)q = \bar{q}\mathcal{D}q . \quad (186)$$

The last equality is the definition of \mathcal{D} and the covariant derivative \mathcal{D} contains the vector and axial-vector external fields. The real part of the effective action in Euclidean space using the heat kernel expansion is then given by ($\epsilon = M_Q^2/\Lambda_\chi^2$):

$$S_{eff} = -\frac{1}{32\pi^2} \sum_{n \geq 1} \Gamma(n-2, \epsilon) (M_Q^2)^{2-n} \int d^4x \text{tr} \mathcal{H}_n(x) . \quad (187)$$

The $\mathcal{H}_n(x)$ are the Seeley-DeWitt coefficients and these are constructed out of E , $R_{\mu\nu}$ and their covariant derivatives. These are defined by

$$\mathcal{D}_E^\dagger \mathcal{D}_E = -D_\mu D^\mu + E + M_Q^2 \quad \text{and} \quad [D_\mu, D_\nu] = R_{\mu\nu} . \quad (188)$$

In terms of the external fields s , p , l_μ and r_ν they are (only terms that can contribute to two-point functions are given):

$$E = i\gamma_\mu \gamma_5 M_Q (r_\mu - l_\mu) - \frac{i}{2} \sigma_{\mu\nu} R_{\mu\nu} + s^2 + M_Q s + p^2 + \gamma_\mu \partial_\mu s - i\gamma_\mu \gamma_5 \partial_\mu p , \quad (189)$$

$$R_{\mu\nu} = -\frac{i}{2} (l_{\mu\nu} + r_{\mu\nu} - \gamma_5 (l_{\mu\nu} - r_{\mu\nu})) . \quad (190)$$

Here we see that E and $R_{\mu\nu}$ vanish for vanishing external fields so only terms containing at most two factors of E and $R_{\mu\nu}$ can contribute to the two-point functions.

The first two coefficients are:

$$\mathcal{H}_0 = 1 \quad \text{and} \quad \mathcal{H}_1 = -E . \quad (191)$$

\mathcal{H}_1 thus contributes to the scalar and pseudoscalar two-point function. These are the only two-point functions that contain a quadratic divergence.

The $\mathcal{H}_{n \geq 2}$ only contain two types of terms that can contribute to two-point functions. Let us look at all possibilities.

Terms with a single E . These are of the form $D^{2(n-1)}E$ and are total derivatives, so they do not contribute to the two-point functions. The same argument applies to terms with a single $R_{\mu\nu}$.

Terms with one E and one $R_{\mu\nu}$. Extra derivatives acting on these can always be commuted, the commutator introduces an extra factor of $R_{\mu\nu}$ and then only contributes earliest to a three point function. We can also use partial integration. All this type of terms can thus be brought into the form

$$D_\mu D_\nu E D^{2(n-3)} R_{\mu\nu} = \frac{1}{2} [D_\mu, D_\nu] E D^{2(n-3)} R_{\mu\nu} . \quad (192)$$

The commutator becomes an extra factor of $R_{\mu\nu}$ so this type of terms does not contribute to two-point functions. We conclude that the $\mathcal{H}_{n \geq 2}$ only contribute to two-point functions through terms like

$$E D^{2(n-2)} E , \quad D_\alpha R_{\alpha\beta} D^{2(n-3)} D_\mu R_{\mu\beta} \quad \text{and} \quad R_{\alpha\beta} D^{2(n-2)} R_{\alpha\beta} . \quad (193)$$

Using Eq. (190) the last two terms are of the form

$$D_\alpha v_{\alpha\beta} D^{2(n-3)} D_\mu v_{\mu\beta} + D_\alpha a_{\alpha\beta} D^{2(n-3)} D_\mu a_{\mu\beta} \quad (194)$$

and

$$v_{\alpha\beta} D^{2(n-2)} v_{\alpha\beta} + a_{\alpha\beta} D^{2(n-2)} a_{\alpha\beta} . \quad (195)$$

So these contribute only to the transverse part and equally for the vector and the axial-vector two-point function. The first term has a part containing $R_{\mu\nu}$ as well. It contributes only to the transverse part, and equally for the vector and axial-vector case.

The remaining type of terms can be rewritten using the explicit form of E .

$$\begin{aligned} \int d^4 x \text{tr} E D^{2(n-2)} E &= N_c \int d^4 x \text{tr} [16M_Q^2 A_\mu \partial^{2(n-2)} A_\mu + 16M_Q A_\mu \partial^{2(n-2)} \partial_\mu P \\ &+ 16M_Q^2 P \partial^{2(n-1)} P + 16M_Q^2 S \left(1 + \frac{\partial^2}{4M_Q^2} \right) \partial^{2(n-2)} S] . \end{aligned} \quad (196)$$

The axial-vector terms contribute only proportionally to $g_{\mu\nu}$. This together with the above contribution leads to:

$$\bar{\Pi}_V^{(0)}(Q^2) = \bar{\Pi}_{(M)}^S(Q^2) = 0 , \quad (197)$$

$$\bar{\Pi}_V^{(1)}(Q^2) = \bar{\Pi}_A^{(1)}(Q^2) + \bar{\Pi}_A^{(0)}(Q^2) . \quad (198)$$

The first two of these equations appear because the vector current in the Lagrangian Eq. (186) is conserved. The third one is the reason why the first Weinberg sum rule is satisfied even at the one-loop level. It also guarantees both Weinberg sum rules after the resummation. Including the contributions from \mathcal{H}_1 we also have

$$-2M_Q \overline{\Pi}_M^P(Q^2) = Q^2 \overline{\Pi}_A^{(0)}(Q^2) , \quad (199)$$

$$2M_Q \overline{\Pi}_P(Q^2) = -2\langle \overline{Q}Q \rangle - Q^2 \overline{\Pi}_M^P(Q^2) , \quad (200)$$

$$\overline{\Pi}_S(Q^2) = \overline{\Pi}_P(Q^2) + Q^2 \overline{\Pi}_A^{(0)}(Q^2) . \quad (201)$$

In Eq. (200) we have used the relation between the coefficient of \mathcal{H}_1 and the quark vacuum expectation value. In the chiral limit this vacuum expectation value is determined uniquely by the contribution of $\mathcal{H}_1 = -E$. This derivation is also valid in the presence of low-frequency gluons. The effective action after including the low-energy gluonic effects through gluonic vacuum expectation values, still has to be constructed out of E and $R_{\mu\nu}$. This was precisely the argument used in Ref. [13] to obtain relations between the low-energy coupling constants that are independent of the gluonic corrections. The results following from the relations (197-201) after resummation are the equivalent relations for the two-point functions. This is what we used in Sect. 3 to rewrite all the two-point functions in terms of essentially two functions and one constant.

The preceding derivation was obtained using the Seeley-DeWitt expansion to all orders. Let us now show how several results can also be obtained from the underlying relations in the Lagrangian (186). These relations are:

$$\partial_\mu (\overline{q} \gamma_\mu q) = 0 , \quad (202)$$

$$\partial_\mu (\overline{q} \gamma_\mu \gamma_5 q) = 2iM_Q \overline{q} \gamma_5 q , \quad (203)$$

$$\{q_\alpha^{a\dagger}(x), q_\beta^b(0)\} = \delta^{ab} \delta_{\alpha\beta} \delta^3(x) . \quad (204)$$

Eq. (204) is valid at equal times. a, b are colour-flavour indices and α, β are Dirac spinor indices.

We start from

$$q_\mu \overline{\Pi}_{\mu\nu}^A = \int d^4x (\partial_\mu e^{iq \cdot x}) \langle 0 | T (A_\mu(x) A_\nu(0)) | 0 \rangle \quad (205)$$

$$= -2M_Q \int d^4x \langle 0 | T (P_\mu(x) A_\nu(0)) | 0 \rangle \\ - \int d^4x \delta_{\mu 0} \delta(x^0) \langle 0 | [A_\mu(x), A_\nu(0)] | 0 \rangle \quad (206)$$

$$= -2iM_Q \overline{\Pi}_\nu^{(P)} . \quad (207)$$

The matrix element of the equal time commutator vanishes for two identical currents. This follows from Eq. (204). Putting in the form of the two-point functions this

leads to

$$q^2 q_\nu \overline{\Pi_A^{(0)}} = 2M_Q q_\nu \overline{\Pi_{(M)}^P} \quad (208)$$

or the same as equation (199). In the full theory we have $\partial_\mu A_\mu = 0$ so the identical derivation leads to:

$$\Pi_A^{(0)}(Q^2) = 0 . \quad (209)$$

This equation is satisfied by the fully resummed two-point function.

A similar derivation leads to

$$q_\mu \overline{\Pi_\mu^P} = 2iM_Q \overline{\Pi^P} - \int d^4x \delta_{\mu 0} \delta(x^0) \langle 0 | [A_\mu(x), P(0)] | 0 \rangle . \quad (210)$$

Here the equal time commutator worked out using Eq. (204) does not vanish. A term proportional to the quark vacuum expectation value remains and leads to Eq. (200). In the full theory $\partial_\mu A_\mu = 0$ so we obtain

$$\Pi_{(M)}^P(Q^2) = -2 \frac{\langle \overline{Q}Q \rangle}{Q^2} . \quad (211)$$

This equation is also satisfied by the fully resummed two-point function.

References

- [1] S. Weinberg, Phys. Rev. Lett. 18 (1967) 507.
- [2] T. Dass, G.S. Guralnik, V.S. Mathur, F.E. Low and J.E. Young, Phys. Rev. Lett. 18 (1967) 759.
- [3] S.L. Glashow and S. Weinberg, Phys. Rev. Lett. 20 (1968) 224.
- [4] M. Gell-Mann, R.J. Oakes and B. Renner, Phys. Rev. 175 (1968) 2195.
- [5] E.G. Floratos, S. Narison and E. de Rafael, Nucl. Phys. B155 (1979) 115.
- [6] C. Becchi, S. Narison, E. de Rafael and F.J. Ynduràin, Z. Phys. C8 (1981) 335.
- [7] D. Broadhurst, Phys. Lett. 101B (1981) 423.
- [8] M.A. Shifman, A.I. Vainshtein and V.I. Zakharov, Nucl. Phys. B147 (1979) 385, 447.
- [9] S. Narison, QCD Spectral Sum Rules, World Scientific Lecture Notes in Physics, Vol. 26.
- [10] J. Gasser and H. Leutwyler, Ann. of Phys.(N.Y.) 158 (1984) 142.
- [11] G. 't Hooft, Nucl. Phys. B72 (1974) 461.

- [12] J. Gasser and H. Leutwyler, Nucl. Phys. B250 (1985) 465.
- [13] J. Bijnens, Ch. Bruno and E. de Rafael, Nucl. Phys. B390 (1993) 501.
- [14] J. Bijnens and E. de Rafael, Phys. Lett. B273 (1991) 483.
- [15] D. Espriu, E. de Rafael and J. Taron, Nucl. Phys. B345 (1990) 22, erratum ibid. B355 (1991) 278.
- [16] J. Donoghue, E. Golowich and B. Holstein, Phys. Rev. D46 (1992) 4076.
- [17] Y. Nambu and G. Jona-Lasinio, Phys. Rev. 122 (1961) 345.
- [18] A. Manohar and H. Georgi, Nucl. Phys. B234 (1984) 189.
- [19] S. Peris and E. de Rafael, Constituent Quark Couplings and QCD in the large N_c limit, preprint CPT-93/P.2883, UAB-FT-310, to be published in Phys. Lett. B.
- [20] G. Ecker, J. Gasser, H. Leutwyler, A. Pich and E. de Rafael, Phys. Lett. B223 (1989) 425.
- [21] S.H. Kahana and G. Ripka, Phys. Lett. B278 (1992) 11.
- [22] J. Bijnens, W.A. Bardeen and J.-M. Gérard, Phys. Rev. Lett. 62 (1989) 1343; G. Ecker, J. Gasser, A. Pich and E. de Rafael, Nucl. Phys. B321 (1989) 311.
- [23] R.D. Peccei and J.Sola, Nucl. Phys. B281 (1987) 1.
- [24] J. Donoghue, B. Holstein and D. Wyler, Electromagnetic Self Energies of Pseudoscalar Mesons and Dashen's Theorem, preprint, UMHEP-376.
- [25] J. Bijnens, Violations of Dashen's Theorem, NORDITA 93/15 N,P, to be published in Phys. Lett. B.

Table 1: Values of the masses determined from the poles in the two-point functions and from the low-energy expansion of ref. [13].

Meson	ref. [13]	Pole
M_V	0.81 GeV	0.70 GeV
M_A	1.3 GeV	0.9 GeV [†]
M_S	0.62 GeV	0.53 GeV = $2M_Q$

[†] In the resummed version there is an strong enhancement around this value of the two-point function. It does not become a pole with the values of the parameters chosen here.

Figure Captions

- Fig. 1: (a): The set of diagrams summed to obtain $g_A(Q^2)$. X is the insertion of the pion field and the other lines are fermions.
(b): The gap equation. The thick line is the full fermion propagator. The thin line is the bare fermion propagator.
- Fig. 2: (a): The set of diagrams to be summed for the two-point functions.
(b): The one loop fermion bubble.
- Fig. 3: The spectral function of the vector two-point function. The full line is the full ENJL result. The dashed line is the result at one-loop. Here $Q = \sqrt{t}$.
- Fig. 4: The real part of the vector two-point function. Plotted are the full result with (labelled gluon) and without (labelled full) gluonic corrections. The VMD parametrization (eff) and the one loop result (1-loop).
- Fig. 5: The real part of the axial-vector two-point function multiplied by Q^2 . The effect of axial-pseudoscalar mixing that the full resummation reproduces is visible at all Q 's. The labels have the same meaning as in Fig. 4.
- Fig. 6: The real part of the pseudoscalar two-point function multiplied by Q^2 . Notice how the resummed version produces the pole at $Q = 0$. The labels have the same meaning as in Fig. 4.
- Fig. 7: Curves for Δm_π^2 in terms of the scale μ . Plotted are the long-distance part for the pion exchange term only (LD-CHPT), the result of ref. [14] (LD-mean) and the ENJL-result after the resummation (LD-ENJL). The short distance contributions are plotted for three values of $\langle \bar{Q}Q \rangle = -(194 \text{ MeV})^3$ (SD194), $-(220 \text{ MeV})^3$ and $-(281 \text{ MeV})^3$.
- Fig. 8: The full result Δm_π^2 versus μ corresponding to the sum of the long distance ENJL result with the short distance evaluation using $\langle \bar{Q}Q \rangle$ as given by the ENJL-model (see text).

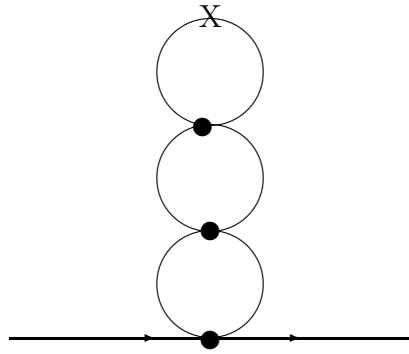


Fig. 1a



Fig. 1b

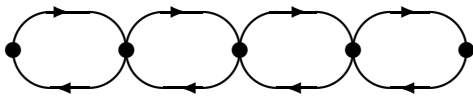


Fig. 2a

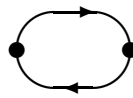
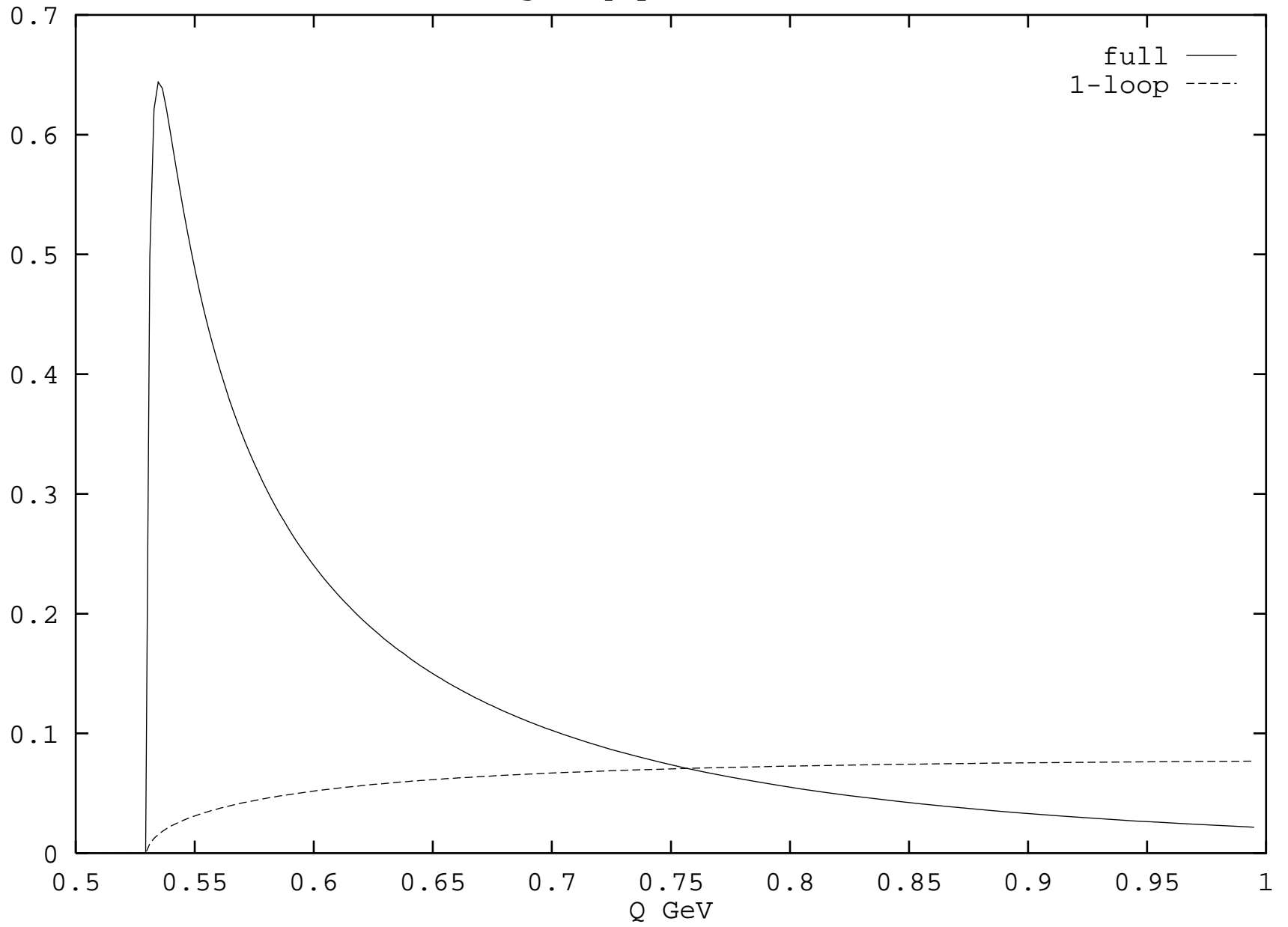
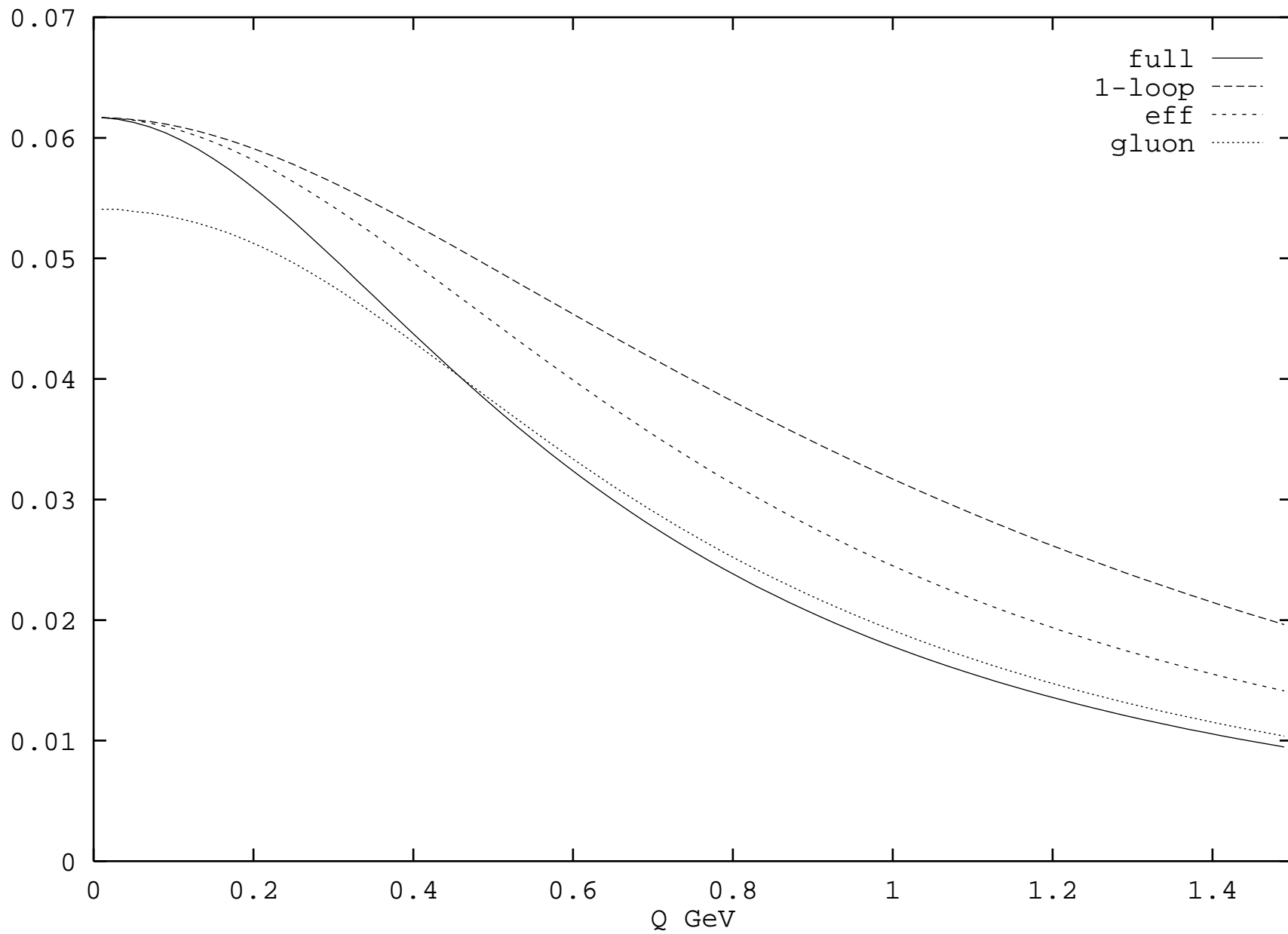


Fig. 2b

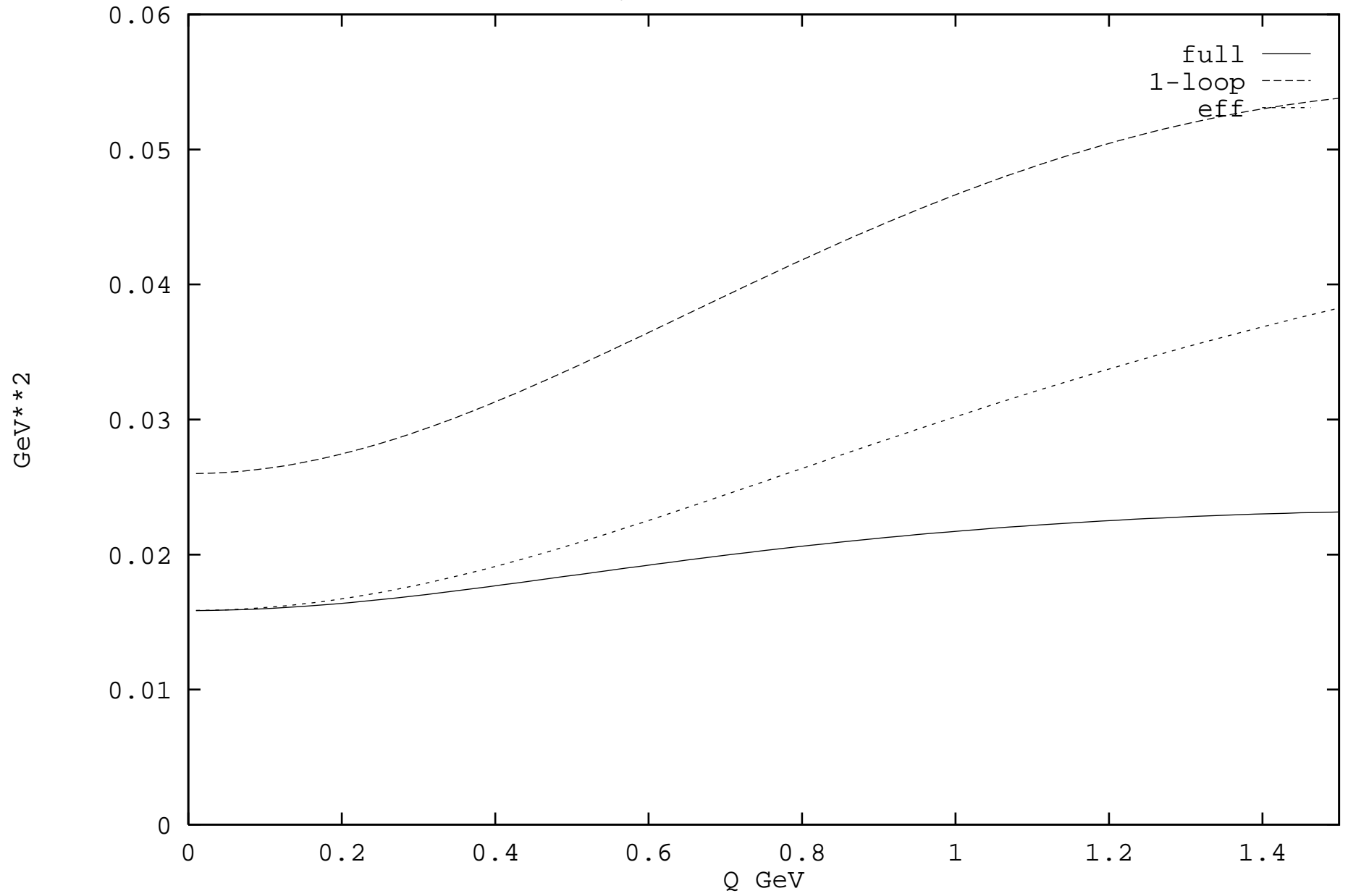
Imaginary part of vector



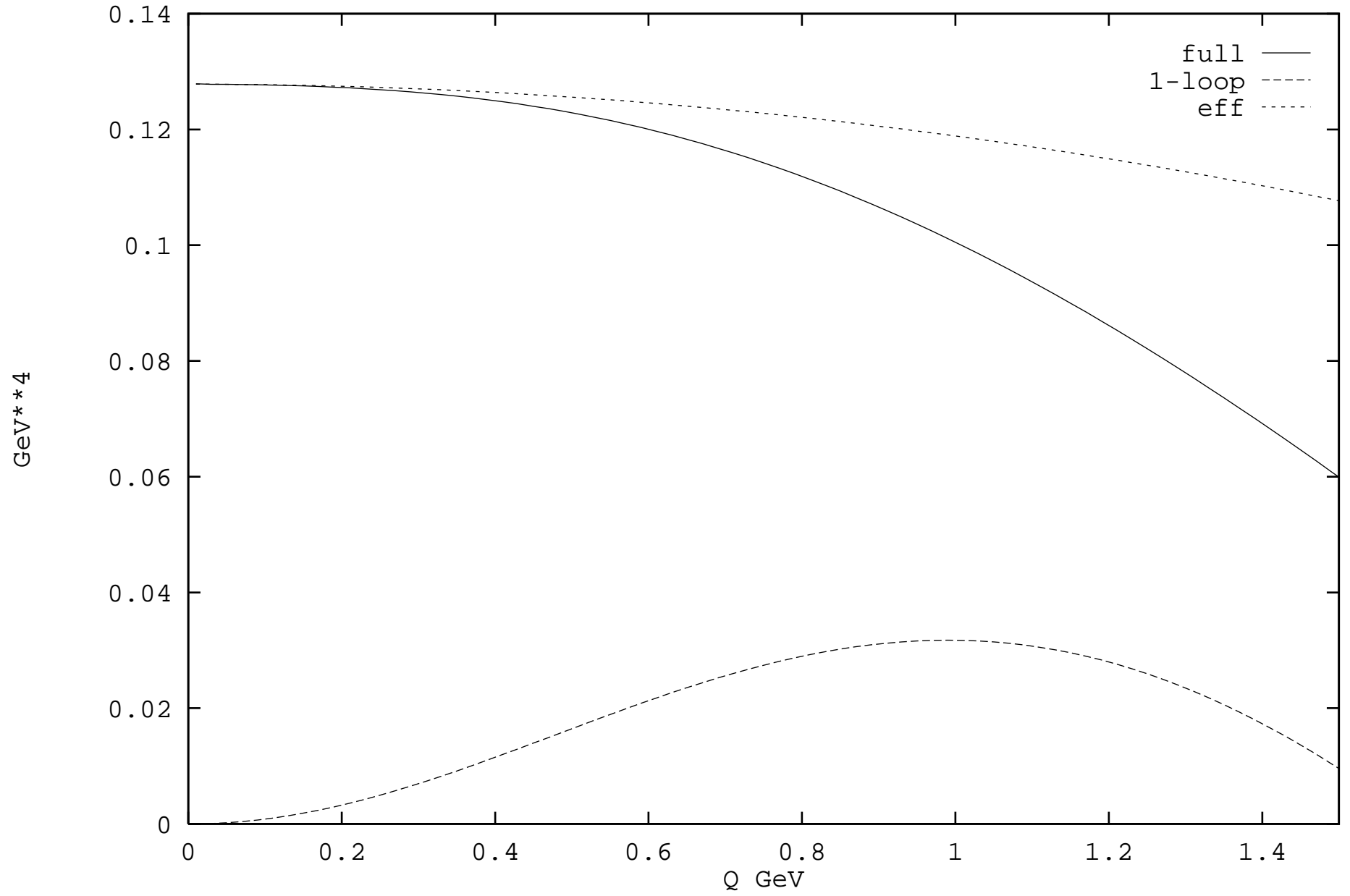
vector



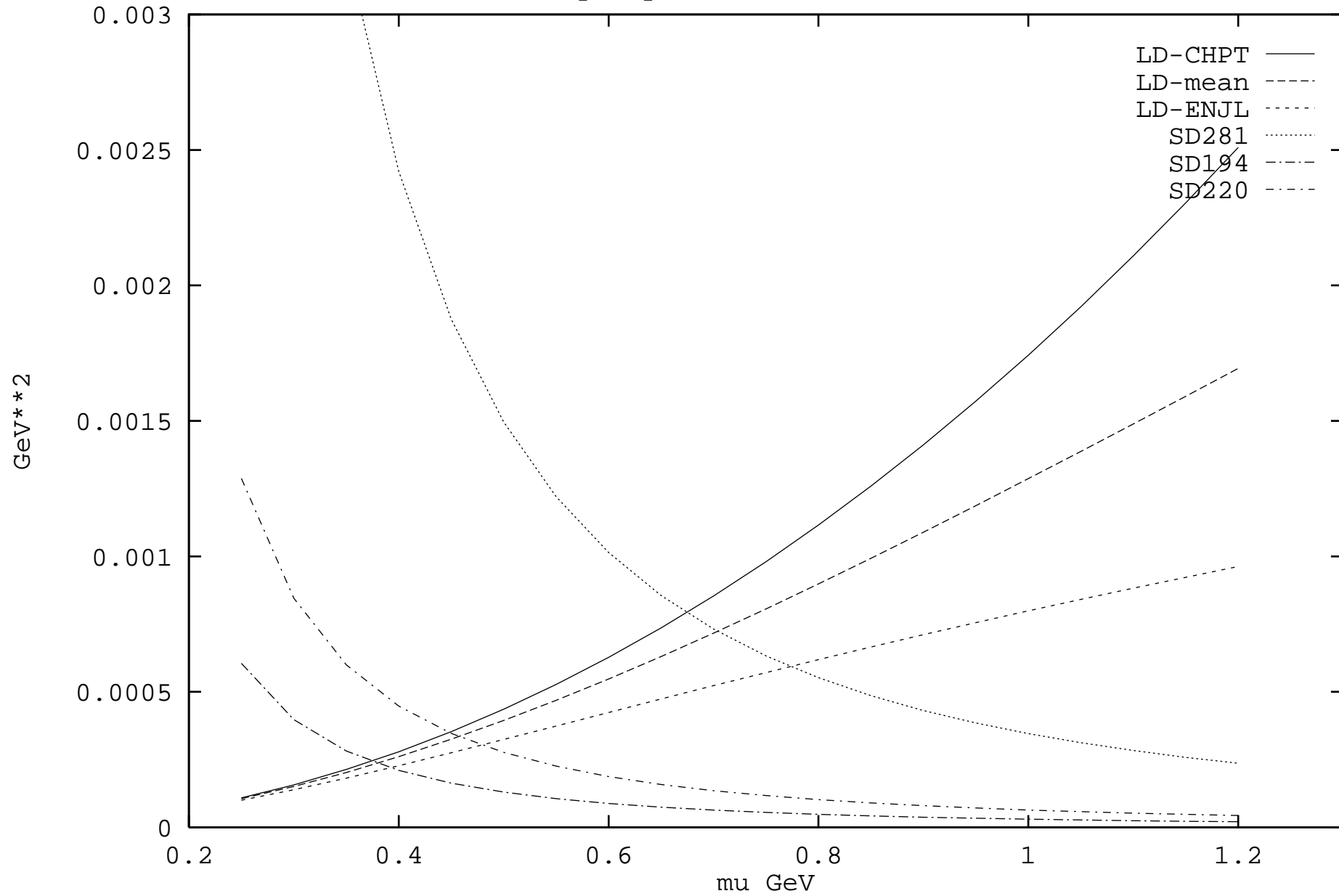
Q^2 * axial-vector



Q^2 * pseudo-scalar



pi+-pi0 mass difference



pi+-pi0 mass difference

